Chemical Engineering Journal 374 (2019) 1153–1179

Contents lists available at ScienceDirect

Chemical Engineering Journal

journal homepage: www.elsevier.com/locate/cej

Review

State-of-the-art materials for high power and high energy supercapacitors: Performance metrics and obstacles for the transition from lab to industrial scale – A critical approach

Joana Monteiro Baptista[a,b,*], Jagdeep S. Sagu[b], Upul Wijayantha KG[b], Killian Lobato[a]

[a] Instituto Dom Luiz (IDL), Faculdade de Ciências da Universidade de Lisboa, Campo Grande C8, 1749-016 Lisboa, Portugal
[b] Energy Research Laboratory (ERL), Department of Chemistry, Loughborough University, Loughborough, Leicester LE11 3TU, UK

HIGHLIGHTS

- Future supercapacitors are anticipated to be hybrid and aqueous-based.
- Production processes require optimization for scale-up of promising prototypes.
- Identification of promising materials and architectures is currently convoluted.
- Non-uniform performance assessment methods preclude accurate benchmarking of devices.

GRAPHICAL ABSTRACT

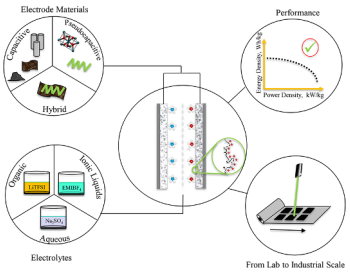

ARTICLE INFO

Keywords:
Supercapacitor
Review
Materials
Performance
Scalability

ABSTRACT

The growing field of supercapacitors has already gained enough maturity and complexity to be the object of highly specific reviews. This review aims to provide a comprehensive outline of the topic, by presenting the state-of-the-art electrolytes and electrode materials used in supercapacitors as well as the relationship between their intrinsic features and their key performance indicators. This analysis is complemented by numerous examples of recent literature-reported performances of hybrid supercapacitors. To aid comparison, these are listed in tables and shown in plots, organized by type of electrode material and by type of electrolyte. Finally, performance differences between lab scale and commercial scale devices are put in perspective, by exploring, on one hand, the obstacles to the transition from promising lab scale to industrial scale devices and by explaining, on the other hand, the reasons why the same type of electrode material and electrolyte combination often perform more poorly in real-world devices. With this approach, the authors expect to give a useful insight (and a comprehensive snapshot) into the challenges that need to be surpassed to bridge the gap between lab scale and industrial scale devices.

1. Introduction

Along with an increasing penetration of renewable energies in the electric system, comes also an increasing need to overcome the high variability of these resources. Moreover, the expected electric vehicle boom will add significant challenges to the operation of the electrical grid [1]. Hence, notwithstanding the importance of demand side management strategies, it is clear that our society is in need of high-performance electricity storage technologies. When speaking of performance, it is crucial to take into consideration the application and the

* Corresponding author.
E-mail address: jpbaptista@fc.ul.pt (J.M. Baptista).

https://doi.org/10.1016/j.cej.2019.05.207
Received 7 February 2019; Received in revised form 25 April 2019; Accepted 28 May 2019
Available online 29 May 2019
1385-8947/

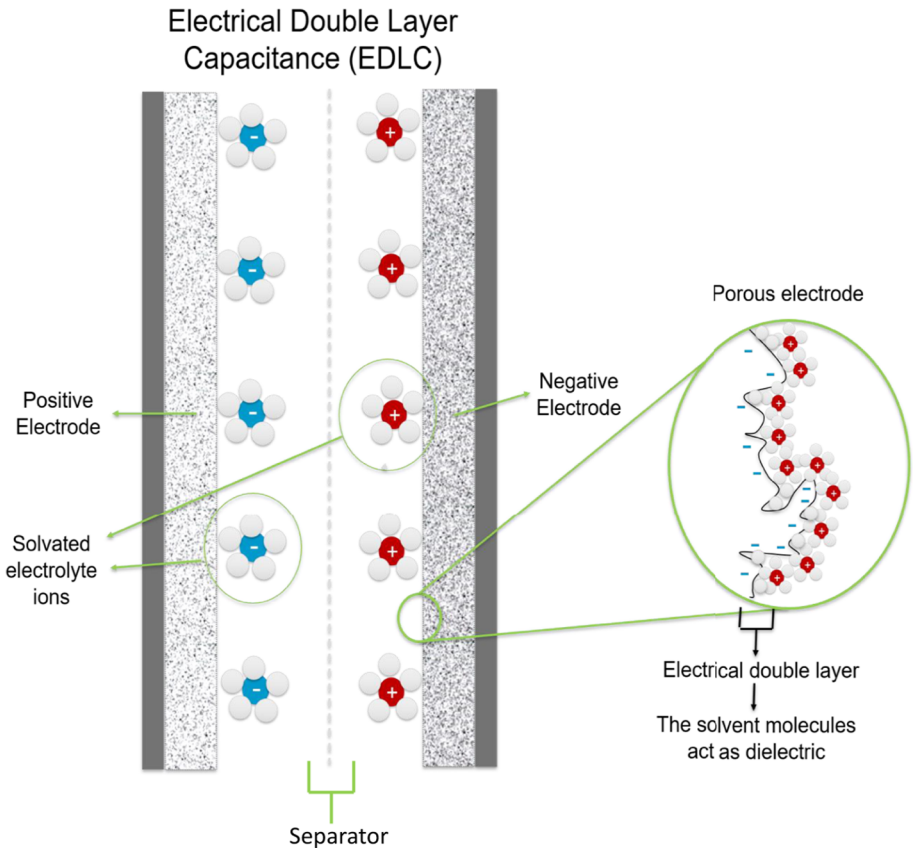

Fig. 1. Simplified schematic illustration of an EDLC. Drawing not to scale.

time scale associated to the energy storage [2]. Currently, the market for medium-term electricity storage is mostly dominated by batteries whilst capacitors are preferred for very small scale and short-term applications (mainly electronics). Supercapacitors lie between these two technologies, providing higher energy densities but smaller power densities than conventional capacitors while simultaneously outperforming batteries in terms of power density and cyclability but lagging behind them in terms of energy density [3].

Thus, supercapacitors are particularly attractive for applications requiring relatively high power and low energy as well as fast and frequent charge/discharge cycles, such as: regenerative braking systems in fully electric vehicles or in heavy hybrids that experience many start/stop cycles during the day (city transit buses, trash trucks, etc.) [4], energy management in microgrids or stand-alone systems [5], portable consumer electronics [6], AC line filtering [7], water desalination systems [8], memory backup systems [9], emergency doors in airplanes [10], wind turbine blade pitch systems [11] and seaport cranes [9].

Given that the demand for supercapacitors for these applications is increasing, there is not an equal transition of lab-scale technologies into the market for real world applications. Carbon-carbon based supercapacitors continue to dominate the commercial market despite the number of breakthroughs made using a wide array of electrode materials and combinations which have resulted in ground breaking power and energy densities for lab-scale devices. The main aim of this review paper is to list the recent state-of-the-art materials and device configurations for supercapacitors with the purpose of understanding why these materials are struggling to be commercialised.

One of the main drawbacks of supercapacitors - when compared to batteries - is their low energy density. Improving this feature (without sacrificing their high power density and cyclability) has been one of the most discussed research topics in this field. In order to comprehend the efforts that have been undertaken towards achieving this goal, one should first understand the fundamental working principles of a supercapacitor (here explained in section 2) and then how the features of the device relate to its performance (section 3). Next, the electrolytes and the electrode materials are addressed, respectively, in sections 4 and 5. Examples of hybrid devices recently reported in the literature are then presented in section 6. Afterwards, building on the fact that most of the best performing lab scale supercapacitors reported in the literature have never reached the market (which, indeed, continues to be dominated by simple and mediocre devices), Section 7 presents some bottlenecks for the transition from lab to industrial scale and on potential strategies to tackle those limitations as well. Finally, Section 8 presents some conclusions and summarizes the discussed topics by pointing out the perceived research directions in the field of supercapacitors.

2. Working principles

Similarly to capacitors, in conventional supercapacitors – often called Electric Double Layer Capacitors (EDLC) – the energy is also stored by the electric field in the dielectric separating the opposing charges [12].

The amount of charge that a parallel plate capacitor can store per unit of potential difference applied to its terminals is defined as capacitance (C, measured in F). According to Eq. (1), it increases with the surface area (A, in m^2) of the plates (as well as with the absolute permittivity of the dielectric material that separates them, "ε", in F/m) and decreases with the separating distance (d, in m) [13] – the distance between the opposing charges, which, in this case, corresponds to the thickness of the dielectric layer.

$$C = \frac{\varepsilon A}{d} \quad (1)$$

The same principles apply to EDLCs, hence explaining their high capacitance: in their case, the "dielectric" is a layer of solvent molecules (which are adsorbed to the electrode's surface and which solvate the ions of the electrolyte hence separating these two charged surfaces) - whose thickness can be as low as 0.3 nm in the case of an aqueous electrolyte [14]. Moreover, EDLCs also present highly porous electrodes, which results in a large surface area ($> 1000\ m^2/g$) [15]. As shown in Fig. 1, there is an accumulation of cations near the surface of the negatively charged electrode and a large density of anions near the surface of the positively charged electrode. Between the electrolyte-soaked electrodes lies the separator which is a membrane highly permeable to the ions of the electrolyte. Its function is to prevent the electric contact and thus electrical shorting between the electrodes [16].

Simply, a supercapacitor can thus be regarded as a series of two capacitors (one at the positive electrode/electrolyte interface and another one at the negative electrode/electrolyte interface). However, in reality, the equivalent electric circuit of a supercapacitor is much more complex, also involving an equivalent series resistance (associated with the intrinsic electronic properties of the electrode matrix and electrolyte solution, mass transfer resistance of the ions in the matrix, and contact resistance between the current collector and the electrode [10]) as well as a parallel resistance associated to self-discharge. Some authors have gone further and tried to develop equivalent electric circuits that could adequately represent a supercapacitor's dynamics in different time-scales. Zubieta and Bonert [17] proposed a model comprising three RC branches, i.e., immediate branch, delayed branch and long-term branch [18]. Other more sophisticated models, such as the transmission line model [19] can be mentioned but their discussion falls outside the scope of this summary.

Besides the electric double layer capacitive mechanism (which is particularly fast and is hence associated to high power densities), there is another one, "pseudocapacitance". Its name arises from the fact that pseudocapacitive materials present an electrochemical signature identical to the capacitors' (i.e. an almost constant differential capacitance, dQ/dV throughout the whole potential window [20] – a feature absent in battery-type materials) but their charge storage is not based on electrostatics. Instead, it is based on fast reversible Faradaic reactions occurring at or near the surface [21]. This mechanism (which renders higher energy densities) is more prone to occurring in electrodes made of transition metal oxides (such as RuO_2 and MnO_2) and conducting polymers (PAni, PEDOT and PPy [22]), but can also take place in carbon-based electrodes, especially when oxygen- and nitrogen-containing groups are present. Pseudocapacitance and double-layer capacitance can (and usually do) coexist in a same material. The overall capacitance is the sum of the double layer capacitance with the pseudocapacitance. Chen [23] presents a comprehensive discussion of these two mechanisms.

The traditional approach was to assemble symmetric supercapacitor cells: two identical electrodes, either made of a purely capacitive material (EDLC) or made of a pseudocapacitive material (the so-called "pseudocapacitors"). However, as pointed out by G. Yu et al. [24], combining these two different types of materials can yield a significant increase in their performance. Therefore, more sophisticated architectures began to arise. There are essentially four types of possible configurations for supercapacitor cells in terms of active electrode materials:

- **Simple symmetric supercapacitors:** two identical electrodes, made of a single active material (e.g. activated carbon // activated carbon)
- **Internal Series Hybrids (ISH):** two different electrodes and each electrode made of a single active material (e.g. RuO_2 // activated carbon); the result is an asymmetric device
- **Internal Parallel Hybrids (IPH):** two identical electrodes, made of at least two different active materials (e.g. MnO_2-graphene // MnO_2-graphene); the result is a symmetric device
- **Double Hybrids (DH):** two different electrodes, each one made of at least two different active materials (e.g. polypyrrole-graphene // MnO_2-activated carbon fibres); the result is an asymmetric device

The term "hybrid" here is used in its broadest sense: any combination of two different things – in particular, two different materials, regardless of their nature (e.g. a device with an activated carbon electrode and a graphene-based electrode, both purely capacitive, would still be classified as "hybrid"). This definition deliberately intends to break free from the inconsistent use of the term hybrid; e.g. the term has been used to classify as exclusively asymmetric devices, or composite based electrodes, or a composite of a pseudocapacitive and purely capacitive materials. With this clarification, devices can therefore be classified according to their electrode arrangement (ISH, IPH and DH). To highlight the coexistence of different charge storage mechanisms, one can simply state that it has both capacitive and pseudocapacitive materials.

The distinction between "pseudocapacitive" and "battery-type" materials [25] is, at times, unclear in the literature. In fact, many authors classify any material that undergoes redox reactions as "pseudocapacitive", which is not in accordance with the original definition given by Conway [20] – for a material to be "pseudocapacitive" it should provide a faradaic charge storage and present an almost constant value for dQ/dV throughout the whole potential range (much like a conventional capacitor). Ruthenium and manganese oxides meet these two criteria, but, for example, nickel and cobalt oxides or hydroxides fail to meet the latter and should hence be classified as "battery-type" materials instead.

The charge–discharge profile can appear pseudocapacitive for a composite electrode made from a purely capacitive material and battery-type material. The same can occur for an asymmetric device where one electrode is made of a capacitive-type material and the other is made of a battery-type material (e.g. Li-ion or Na-ion capacitor [26,27]). However, it is worth stressing that these pseudocapacitive behaviours happen at a "systemic" level and not at the material level. The term "supercapattery" introduced by Chen [23] aims to clarify the definition of devices that combine rechargeable battery and supercapacitor materials. Recently, Chen and Xue have proposed a particular type of supercapattery electrode materials - colloidal electrodes – which can provide multiple-electron redox reactions at relatively fast discharge–charge rates and which lead to a more efficient use of the electrode materials [28]. In a colloidal electrode, metallic ions and ion clusters dispersed throughout a conductive substrate (e.g. carbon cloth) interact with each other in a highly complex system, with a large surface-to-volume ratio [29]. The "cation source" is typically a hydrated salt (e.g. $Fe(NO_3)_3{\cdot}9\ H_2O$ [30]), which is mixed with a binder, a conductive additive and a solvent. The current collector is then coated with the resulting slurry and, after dried and compressed, the electrode is finally cycled in an alkaline solution. At the electrode–electrolyte interface [31], several cations attached to the colloidal electrode by ligands (mostly OH^- and H_2O) are formed and act as electroactive centres. It is largely accepted that colloids present a good strategy to obtain high energy and high power density supercapatteries [31–35].

3. Performance

The main performance indicators in supercapacitors are capacitance, energy density (which also depends on capacitance), power density and cyclability. Except for the latter, more often all the other indicators can be expressed per unit of mass, per unit of volume and sometimes even per unit of footprint area. Usually, gravimetric/volumetric energy and power densities referred to in the literature are obtained as the ratio of the delivered energy or power to the mass/volume of the active materials in the electrode.

This practice, despite enabling a fairer comparison between

different materials, largely overestimates the performance that a certain device would present in a real-world application, where other non-active materials (e.g. binders, current collectors, separator, package, cell assembly components, etc.) are inevitably present and add mass and volume to the supercapacitor. Obreja [36] argues that, for a lab device with a certain gravimetric performance, the energy and power densities of an optimised practical supercapacitor cell using that same technology would be less than half.

In addition, care should be taken while comparing literature-reported results, since some of them refer to the performance of a whole supercapacitor (two-electrode configuration) whilst others are obtained from three-electrode cell measurements (and hence only characterize a single electrode). The measurements provided by the former are more likely to resemble the performance of the device in a practical application, but provide less detailed information about the system, since the behaviour of each one of the electrodes is undistinguishable. Ideally, each electrode should be tested in a three-electrode configuration (in order to determine the potential window and identify the presence of any surface functionality) and then the already assembled supercapacitor device should be tested again in a two-electrode configuration.

The measurement techniques more often used to electrochemically characterize supercapacitors (either in a two- or three-electrode configuration) are Cyclic Voltammetry (CV), galvanostatic Charge-Discharge tests (CD) and Electrochemical Impedance Spectroscopy (EIS).

Correctly characterizing the behaviour of a supercapacitor cell or electrode should be the first concern of anyone willing to improve the performance of these devices. Yet, despite the existence of standardized procedures to test commercial devices [37], there still seems to be a lack of consistency in the literature-reported methods used to test lab-scale supercapacitors. Since the obtained results are highly dependent on the measurement conditions (mass loading of electrodes[1], voltage range, charging rates, etc.), it is advisable to follow the recommendations provided by Stoller and Ruoff [38].

3.1. Capacitance

According to Eq. (1), capacitance is inversely proportional to the distance that separates the opposing charges (which, in the case of supercapacitors, is the thickness of the double-layer) and directly proportional to the absolute permittivity of the "dielectric" (again, the double-layer in this case) and to the surface area of the electrodes. So, in principle, to a first degree, the greater the surface area, the greater the capacitance. However, large surface areas are achieved by using highly porous materials and, when the pore size is not adequately matched to the radius of the solvated ion, those pores are not accessible and hence do not contribute to capacitance. In other words, an electrode that presents a high micro porosity (and hence a very large surface area) does not necessarily lead to a very high capacitance. This means that what is relevant is the surface area that is *accessible* to the electrolyte.

Numerous studies have analysed the relationship between the size of the electrolyte ions, the pore size distribution in carbon electrodes and the achieved capacitance. Although there are still some research gaps on this topic, a very important achievement was the ability to produce templated carbons with controlled pore size distributions and optimized interconnectivity. In particular, the emerging class of Hierarchical Porous Graphitic Carbon (HPGC) – which contains micro (1–2 nm), meso (5–50 nm) and macropores (60–100 nm) in a highly organized structure – appears to be very promising. According to Wang et al. [39], who managed to obtain HPGC materials with high energy and power densities in both organic and aqueous electrolytes, the three types of pores can (if carefully architectured) contribute to an enhanced capacitance: macropores act as ion-buffering reservoirs, mesopores reduce the ion-transport resistance and micropores enable charge accommodation. Contrary to the previous belief, some authors (such as Gogotsi and co-workers [40]) have shown that even the micropores whose size is smaller than the solvated ion - though obviously not smaller than the de-solvated ion – can be accessible to the electrolyte giving rise to high capacitances. Nevertheless, this is only true if the ion loses or distorts its solvation shell, which might happen or not, depending on the pore geometry, on the applied voltage [41] and on the nature of the electrolyte and electrode material.

Moreover, some authors (namely Huang and co-workers [42]) have shown that Eq. (1) – originally developed for parallel-plate capacitors – is only suitable for macropores. For meso and micropores different equations were suggested (Eqs. (2) and (3), respectively) with a greater correspondence with experimentally determined capacitances.

$$C = \frac{\varepsilon}{b \ln[b/(b-d)]} A \tag{2}$$

$$C = \frac{\varepsilon}{b \ln(b/a_0)} A \tag{3}$$

where, ε is the absolute permittivity of the electrolyte (in F/m), A is the specific surface area of the electrode accessible to the electrolyte ions (in m^2), b is the pore radius (in m), d is the distance of approaching ions to the surface of the carbon electrode (in m) and a_0 is the effective size of the counterions (in m).

These equations model the relationship between capacitance and some intrinsic features of the supercapacitor. Device capacitance can be determined by cyclic voltammetry (CV), galvanostatic charge discharge (GCD) and electrochemical impedance spectroscopy (EIS). However, capacitance determined by GCD more closely resembles real-world device functioning.

It should be stressed that pseudocapacitance also contributes largely to the overall capacitance of the device. Therefore, besides maximizing double-layer capacitance through the adequate matching between the pore and the ion sizes, it is also advantageous to employ pseudocapacitive materials (such as metal oxides and conducting polymers) and/or oxygen- or nitrogen-containing surface functional groups [43].

3.2. Energy density

Combining the definition of electric force, electric potential difference, current and work, one can deduce that the energy (E) stored within a supercapacitor is given by Eq. (4):

$$E = i \int_{t_2}^{t_2} dU(t) dt \tag{4}$$

where t_1 and t_2 are, respectively, the instant when the capacitive[2] voltage drop begins and the instant when the cell voltage reaches 0 V; i is the discharge current (constant in a galvanostatic CD test) and $dU(t)$ is the infinitesimal voltage drop that occurs during the infinitesimal period dt

When the cell voltage varies linearly with the discharge time – which is the case for an ideal EDLC[3] – and knowing the definitions of current and capacitance, we have:

$$E = \frac{1}{2} C \Delta U^2 \tag{5}$$

where C is total capacitance of the supercapacitor cell (which should

[1] Mass of active materials divided by the electrode's footprint – often expressed in mg/cm^2.

[2] non-resistive – in a CD test, after the current is inverted, an immediate voltage drop appears, due to the equivalent series resistance of the device.

[3] However, this is not true when pseudocapacitance is present nor when the EDLC is discharged with high current densities. Therefore, whenever possible, Eq. (4) should be used instead of Eq. (5).

not be confused with the capacitance of the electrode), in F, and ΔU is the cell voltage, in V.

The significance is that, in order to obtain high energy supercapacitors, the adopted strategy should be to increase the capacitance (following the above-mentioned approach) and, even more importantly, to increase the operating voltage window of the supercapacitor cell since the stored energy is proportional to its square.

Although capacitance is mainly related to the electrode features, it is also dependent on the electrolyte composition. The operational voltage window is highly dependent on electrolyte composition, but also, to a certain extent, dependent on electrode characteristics. This is discussed in further detail ahead.

In general, it is considered that the maximum operating voltage of a supercapacitor is limited by the voltage stability window of the electrolyte, assuming that the electrode material is stable within the potential range (which is the case for carbon–carbon supercapacitors). This is the main reason why, in commercial supercapacitors, organic electrolytes are typically favoured over their aqueous counterparts [44]: water at RTP undergoes electrolysis at approximately 1.23 V [45], which is low when compared to organic electrolytes which are stable up to ca. 2.7 V.

Yet, despite enabling higher operating voltages, organic electrolytes present some significant disadvantages as well, namely toxicity, difficult industrial processing, flammability and cost [15]. Furthermore, due to the larger size of the solvent molecules, the solvated ions have a reduced mobility leading to a higher equivalent series resistance (ESR) [46] – and a reduced accessibility to the electrode micropores [47] (which in turn decreases the capacitance of the device). Moreover, the wettability of carbon electrodes by organic electrolytes is usually lower than for aqueous electrolytes. This in turn affects the penetration of the non-aqueous electrolytes in the electrode pores [10] and thus also contributes to a reduced capacitance.

Given the inherent limitations of non-aqueous electrolytes, significant effort has gone into overcoming the low operational voltage window associated to the aqueous electrolytes. In fact, the operational range can be extended through a careful tuning of the electrode material and of the electrolyte pH [48] – e.g. Wessels et al. [49] reported voltages as high as 2.3 V in a 5 M aqueous solution of $LiNO_3$. Various attempts followed, some of them by using electrode materials of high overpotentials for oxygen and/or hydrogen evolution [50] in asymmetric configurations [51,52]. However, none succeeded in reaching higher voltages. Bichat and Piñero were able to push the limit to 2.4 V, using a supercapacitor composed of carbon electrodes obtained through the pyrolysis of seaweed at 600 °C and a Na_2SO_4 electrolyte [48]. The authors argued that this result was, firstly, due to the influence of the surface functionalities present in the carbon electrodes and secondly, due to the neutral nature of the electrolyte.

More recently, Tomiyasu et al. [50] reported a remarkably high 3.2 V supercapacitor containing a saturated aqueous solution of sodium perchlorate (SSPAS). A graphite mixture (80 wt% graphite, 10 wt% acetylene black and 10 wt% carbon felt) doped with MnO_2 was used as the positive electrode and the same graphite mixture doped with Fe_3O_4 was used as the negative electrode, leading to a high capacitance. The device also presented a notably high energy density (36.3 Wh/kg), explained by the combination of a high capacitance with an unusually large voltage window (allegedly due to the very high concentration of the electrolyte and to the consequent weakening of the hydrogen bond between the water molecules). Fig. 2 illustrates the structure of the supercapacitor where this physical process occurs.

3.3. Power density

The maximum power (P) that theoretically can be delivered by a supercapacitor is given by Eq. (6) [20]:

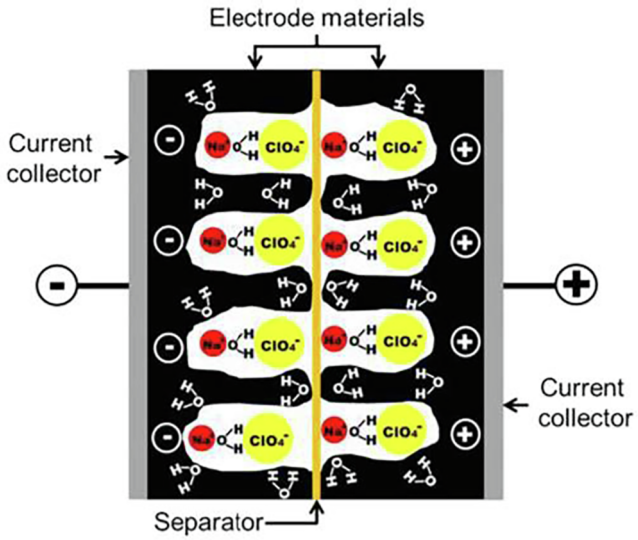

Fig. 2. Schematic structure of a supercapacitor using a saturated aqueous solution of sodium perchlorate as the electrolyte. At least one water molecule should be strongly hydrated to $NaClO_4$. Reprinted from Scientific Reports, Vol 7, H. Tomiyasu et al., An aqueous electrolyte of the widest potential window and its superior capability for capacitors [50], 45048; DOI: https://doi.org/10.1038/srep45048 (2017), Licensed under CC BY 4.0.

$$P = \frac{\Delta U^2}{4R} \tag{6}$$

where ΔU is the maximum cell voltage of the device and R is its ESR.

Similarly to what happens with the energy density, the power density of a supercapacitor is also greatly influenced by its voltage window. Thus, one way of promoting higher power densities is adopting the measures described in the previous section to increase the maximum voltage of the device.

In addition, one can also decrease the ESR. This parameter depends both on the contact resistance between the electrode and the current collector and on the internal resistance of the electrodes [53], which, in turn, is not only associated to the resistivity of the electrode material(s) but also to its morphology, since it strongly influences the diffusion of the electrolyte ions within the electrode matrix. For example, Du and co-workers managed to significantly reduce the ESR and obtain a supercapacitor with a specific power density of 30 kW/kg [53]. The device's high performance was attributed to the fact that the electrodes were based on multi-walled carbon nanotubes thin films (which are highly conductive). Moreover, since no binder was required, the contact resistance between the electrode and the current collector was also smaller. Building on previous insights, Gruner et al. [54] more than doubled the afore-mentioned power density, by producing printable thin-film supercapacitors using Single-Walled Carbon Nanotubes (SWCNT) as electrode materials and an organic electrolyte. The devices attained 70 kW/kg, which is a value comparable to non-printable devices. A few years later, Izadi-Najafabadi et al. reported electrodes capable of delivering 990 kW/kg [55]. This remarkable performance was achieved by use of a novel composite material, made of SWCNT and Single-Walled Carbon Nano Horn[4] (SWCNH), which enabled faster ion transport.

As previously mentioned, both the energy density and the power density depend on the square of the voltage. Accordingly, widening the operating voltage window is critical to enhancing performance [9]. Additionally, an increase in the capacitance will benefit the energy density of the device whereas a reduction of the ESR will promote a

[4] A [carbon] Nano Horn is a horn-shaped sheath aggregate of graphene sheets.

higher power density. However, achieving both in tandem is challenging because for higher currents (i.e. higher power densities), the specific capacitance of the device is reduced and thus, so is its energy density because the supercapacitor cannot fully charge within the short time scales.

In general, purely capacitive materials (mostly carbon-based) are more prone to enabling higher power densities – their charge/discharge rate is mostly limited by the diffusion of the electrolyte ions within the electrode matrix and this diffusion can be enhanced in highly organized structures, such as HPGC. On the other hand, pseudocapacitive materials, due to the redox reactions undergone at their surface, are more likely to result in higher energy densities [56]. The current trend seems to be the association of these two types of materials in order to obtain "the best of both worlds". Electrode materials are discussed in Section 5 and further information on hybrid supercapacitor performances are presented in section 6.

3.4. Cyclability

Cyclability is the ability to withstand a significant number[5] of charge/discharge cycles without a significant capacitance reduction – which can result from the electrolyte evaporation and/or from the degradation of the electrode structure (mainly in pseudocapacitive electrodes). Having a high cyclability is fundamental to ensure competitiveness against batteries[6]. This indicator is assessed by performing a large number of charge/discharge cycles (usually no < 10 000) and then computing the corresponding capacitances. Despite some noteworthy exceptions (e.g. Sagu et al. [57]), supercapacitors based on metal oxides or conducting polymers typically display a lower cyclability than those based on carbon materials.

Some studies (such as the one conducted by Hercule et al. [58]) have focused on increasing the cyclability of non-carbon materials. In this case, this was achieved through the association of two different materials (MoO_2 and $Co(OH)_2$) that, despite presenting a fairly low cyclability when used separately, can – thanks to a synergistic effect – present a more than two-fold increase in their cyclability when combined. Indeed, MoO_2 films, being highly absorptive [59], tend to swell and pulverize causing a fast degradation of the electrode structure. Co $(OH)_2$, nanoflakes, on the other hand, having a large interlayer spacing, tend to collapse easily. Combining these two materials in a hierarchical nanostructure results in an improved electrode which does not present the afore-mentioned problems but retains the original advantages of each of the materials (the good electronic conductivity of MoO_2 and the large interlayer spaces of $Co(OH)_2$).

Other examples include the combination of graphene and metal [hydro]oxides [60] and/or conducting polymers. Since the low cyclability of conducting polymers is mostly due to continuous swelling and shrinking during charging and discharging [56], combining them with graphene is an effective way of increasing their mechanical stability as well as their conductivity and consequently extend their cycle-life [61]. Some nanostructured and multifunctional binders were shown to improve the cyclability of battery electrodes [62] and could do the same in metal oxide or conducting polymer-based supercapacitor electrodes. Yet, there is still room for improvement and significant effort is now dedicated to increasing the cyclability of pseudocapacitive materials.

[5] A supercapacitor that can bear 10 000 cycles with a capacitance reduction of only 1% can be considered to have a good cyclability. Most of commercial carbon-based devices can reach more than 500 000 cycles [162] before reaching 70% of their initial capacitance (which is typically considered to be the end of their useful life).

[6] The majority of batteries do not withstand and more than 1 000 cycles. However, since their cost per Wh is significantly lower (although this is not true for the cost per kW), cyclability is an important factor when comparing the economic performance of these two alternatives.

The overall performance of a supercapacitor is ultimately determined by its architecture, by the features of the materials that constitute its electrodes [34] and by the characteristics of its electrolyte. Therefore, the first step in solving the aforementioned challenges is to understand their relationship with the supercapacitor's structure and components.

4. Electrolytes

The electrolyte composition and its corresponding electrochemical stable potential window (ESPW) play a significant role in determining the power and energy densities of a supercapacitor since both of these indicators are proportional to the square of the voltage. It is for this reason that the majority of commercialized supercapacitors have an organic electrolyte. Usual examples are tetraethylammonium tetrafluoroborate ($TEABF_4$) in acetonitrile (ACN) or in propylene carbonate (PC). These allow for stable operation voltages between 2.5 V and 2.8 V. Nevertheless, there are also other important performance aspects influenced by the electrolyte [63], namely:

a) **the cycling stability** (which depends on the interaction between the ions and the electrode material as well as on the stability of the electrolyte);
b) **the operational temperature range** (which depends on the salt solubility and also on the boiling and freezing points of the electrolyte);
c) **the specific capacitance** (as already mentioned, it depends on the adequate matching between the ion and the pore size distribution);
d) **the ESR of the supercapacitor cell** (which is largely influenced by the ionic conductivity in the bulk electrolyte and by the ion mobility within the electrode structure).

Electrolytes can be grouped according to different criteria, but the most usual are physical state (liquid, solid-state or quasi-solid state) and solvent nature (organic, aqueous or inexistent – which is the case of ionic liquids).

4.1. Aqueous electrolytes

Aqueous electrolytes have recently received increased attention. They are low cost, environmentally benign, highly conductive, and also enable higher specific capacitances because of the smaller radii of the solvated ions.

Although the temperature range of aqueous based electrolytes is limited to water's freezing and boiling points (which may be problematic for some applications), the main disadvantage of aqueous electrolytes is restricted to a narrow operating voltage window (~1.2 V). This is because water electrolysis can initiate, for example, at 1.23 V under standard conditions.

However, as discussed by Zang et al. [64], several strategies have been used to extend the operational voltage window of aqueous electrolytes. One example is to modify the electrode/electrolyte interphase by using super concentrated electrolytes, which quenches water electrolysis whilst also reducing water availability (e.g. Tomiyasu et al. [50]). This will be further discussed in the subsection 4.5. Another strategy is to use materials with a high hydrogen evolution overpotential for the negative electrode (most carbon-based materials display this characteristic) and a material with a high oxygen evolution overpotential for the positive electrode [65]. Asymmetric supercapacitors (devices made by assembling two different electrodes which are stable in complement voltage windows) have attracted significant attention because of this possibility. Finally another strategy is to use pH neutral electrolytes, which reduce the availability of H^+ and OH^- in the solution. Successful examples can be found in Hwang et al. [66] and in Wu et al. [67]. Also, pH neutral electrolytes are less corrosive, and as such the choice of current collector and packaging materials is less

restrictive [63].

Acidic electrolytes typically have higher conductivities (1 M of H_2SO_4 can reach 0.8 S/cm, at 25 °C [68]) when compared to their neutral counterparts and this results in lower ESR values and higher capacitances. Another advantage is that they can promote pseudocapacitive effects in carbon-based electrodes with surface quinone-type functionalities which would be residual in alkaline media [51]. However, some pseudocapacitive materials have been reported to be unstable in acidic electrolytes, which ultimately translates into reduced cyclability.

4.2. Organic electrolytes

Solvents typically used for organic electrolytes are acetonitrile (ACN) or propylene carbonate (PC). Some of the most common salts are tetraethylammonium tetrafluoroborate ($TEABF_4$), spiro-(1,1′)-bipyrrolidinium tetrafluoroborate (SBP-BF4), lithium perchlorate ($LiClO_4$) and lithium hexafluorophosphate ($LiPF_6$) [63]. Organic electrolytes can also be found in a quasi-solid state (organogel electrolytes), which are composed of a polymer host and an organic electrolyte. In particular, the copolymer poly(acrylonitrile)-b-poly(ethylene glycol)-b-poly(acrylonitrile) (PAN-b-PEG-b-PAN), when soaked in a solution of dimethylformamide (DMF) dissolving $LiClO_4$, was shown to have a high ionic conductivity of 10 mS/cm [69].

The main advantage of this type of electrolyte is their wide electrochemical stable potential window (ESPW) – typically 2.5–2.8 V. They also tend to be less corrosive and, as such, cheaper Al current collectors can be used. These advantages are undoubtedly responsible for the fact that the vast majority of commercial supercapacitors use organic electrolytes. Most use ACN because of its high thermal stability, low viscosity and consequently high conductivity [63]).

On the other hand, organic electrolyte's toxicity, flammability and volatility and relatively high cost (linked to their more complex processing and purification) are problematic. Moreover, their lower conductivities and pore accessibility (due to increased size of the solvent molecules) result in a decreased specific capacitance [20]. S. Ahmed et al. [70], assembled four symmetric supercapacitors, all of them having identical electrodes (activated carbon derived from pea skin) but soaked in different electrolytes: one organic (1 M $LiClO_4$ in Ethylene Carbonate (EC)/PC) and three aqueous (1 M H_2SO_4, 1 M Na_2SO_4 and 6 M KOH). The specific capacitances were higher for acidic electrolyte devices; whereas the highest energy and power densities were obtained for the organic electrolyte devices. Yet, this does not indicate that organic electrolytes always lead to higher energy densities. Assuming typical operating voltages for aqueous and organic based devices respectively, the energy density of an aqueous based device can be higher if its specific capacitance is at least ca 7.3 times greater than the specific capacitance[7] of an organic based device. This scenario is feasible due to the greater pore accessibility of aqueous electrolytes, as mentioned beforehand.

4.3. Ionic liquids

Their main attraction lies in the large, up to 6 V, electrochemical potential stability window [71]. Furthermore, they tend to be more thermally stable and have extremely low vapour pressures. Ionic liquids are typically composed by a large asymmetric organic cation and an inorganic or an organic anion [72,73]. Generally, there are five main types of cations for ionic liquids: imidazolium, pyrrolidinium, tetraalkylammonium, piperidinium and pyridinium ions. Anion examples are halides (such as Cl^-, I^- or Br^-) or can be complex ions such as tetrafluoroborate, hexafluorophosphate, cyanate and thiocyanate. Both the cation and anion contribute to the overall properties of the ionic liquid, so these can be customized by cation and anion selection. Fletcher et al. [74] and Van Aken et al. [75] discuss in detail ionic liquid composition and formulation. Some of the most commonly used examples of ionic liquids for supercapacitors are 1-Ethyl-3-methylimidazolium tetrafluoroborate ([EMIM][BF_4]) and 1-Butyl-3-methylimidazolium tetrafluoroborate ([BMIM][BF_4]).

However, ionic liquids are costly and suffer from poor conductivities (usually it does not exceed 14 mS/cm^2 – 50 times lower than 1 M H_2SO_4 aq.). Low conductivity is a result of high viscosity and low ion mobility which translates into high ESR in devices. Preventing water contamination is also a challenge, and, when present, considerably reduces the voltage window [76].

Recently, Thangavel et al. [77] reported ionic liquid supercapacitors with an operating voltage window of 4 V, and notable power and energies densities of 20 kW/kg and 35 Wh/kg respectively. Although with a slightly narrower voltage window of 3.5 V, Wang et al. [78] achieved even higher power and energy densities of 61 kW/kg and 56 Wh/kg respectively. This higher performance is attributed to the electrode design, which was composed of interconnected carbon nanocages forming a carbon nanomesh.

4.4. Electrolytes for solid state/flexible supercapacitors

Due to the increased demand for flexible and wearable electronics, solid and quasi-solid-state electrolytes started to be used in supercapacitors. There are two main types of solid-state electrolytes: dry polymer and gel polymer. An example of a dry polymer electrolyte is LiCl in PEO, and an example of a gel polymer electrolyte is $H_2SO_{4(aq)}$ in PVA. Inorganic solid materials (Li_2S-P_2S_5 glass–ceramic electrolyte [79] and $LiClO_4$-Al_2O_3 [80], for example) can also be used, but reports are uncommon [63]. These solid electrolytes render encapsulation for liquid retention and also act as the separator between electrodes, hence potentially simplifying device manufacture. However, their drawbacks are their inherent low pore penetration – which reduces capacitance – and the existence of ionic conductivity – mechanical stability trade-off. For example, high conductivity gel polymer electrolytes are mechanically fragile, resulting in internal electrical shorting between the electrodes. Their operating temperature range is also limited. On the other hand, dry polymer electrolytes are more stable but have a lower ionic conductivity.

4.5. Recent trends in electrolytes

Redox-active electrolytes and water-in-salt electrolytes are also recent trends.

Redox-active electrolytes are those which contain redox mediators which are electrochemically active in the potential window of operation and, as such, charge transfer occurs between the surface/electrolyte interface, reducing or oxidizing the redox species [63]. Thus, if the reacted species remain confined within the electrode pores and subsequently undergo the reverse redox electrochemical reaction, then this can be considered a form of pseudocapacitive charge storage, occurring now on the electrolyte side of the electrode interface. If, however, the reacted species exit the pores and diffuse to the opposing electrode, these will undergo the reverse electrochemical redox reaction, short circuiting the charge storage process.

Examples of redox mediators are the organic hydroquinone (HQ) [81], indigo carmine [82], sulfonated polyaniline [83] and methylene blue [84] – or inorganic species, e.g. ferrocyanide-ferricyanide redox couple [85]. These can be used in aqueous, non-aqueous and in solid-state electrolytes. Despite the advantage of enabling an increased capacitance and energy density, some of these species (particularly HQ) are also associated to increased self-discharge, apparently due to the migration of the redox-active species between the electrodes.

[7] Energy density is given by $E_{aq} = \frac{1}{2} C_{aq} \Delta U_{aq}^2$ and $E_{org} = \frac{1}{2} C_{org} \Delta U_{org}^2$. Assuming $\Delta U_{aq} = 1V$ and $\Delta U_{org} = 2.7V$, then for $E_{aq} > E_{org}$ to be true, $C_{aq} > 7.29 C_{org}$.

An example of two successful strategies to reduce self-discharge is reported by Chen et al. [86]. Here, self-discharge occurred because p-benzo- quinone (BQ) – an oxidation product of HQ – diffused across the cellulose acetate separator and reached the surface of the cathode where it underwent reduction. Firstly, to stop HQ migration, the original separator was replaced by one that is impermeable to BQ, namely Nafion®. Also successfully demonstrated was the replacement of the redox mediating species by $CuSO_4$ in H_2SO_4. In this case Cu^{2+} reduces to Cu and electrodeposits on the negative electrode upon charging and thus becomes immobile.

Another recent trend is the water-in-salt electrolytes. Instead of having an aqueous matrix where a salt is dissolved, the salt is actually more abundant than the water in these super concentrated solutions. The electrochemical interface region is significantly different. The ions, instead of being completely solvated by the solvent, are mostly surrounded by their counter ions and only a limited number of water molecules. A solid-electrolyte interphase is then formed and passivates the electrode surface. Dubouis et al. [87] focused on understanding the mechanism behind the formation of the fluorinated interphase when the Bis(trifluoromethane)sulfonimide ion ($TFSI^-$) is present. The authors found that these anions could chemically react with the hydroxides generated during the HER and catalyse the formation of a protective layer that prevents further water reduction. As such, operating voltages of up to 3 V are possible [88], which are in the same range as in ionic liquids. These water-in-salt electrolytes have the added advantage of cost and safety when compared to ionic liquids [89].

Lannelongue et al. [90] recently studied the influence that electrolyte molality has on the overall performance of symmetric supercapacitors with activated carbon electrodes and LiTFSI electrolyte. The authors reported a 2.4 V operating voltage window for a 31.5 mol/kg electrolyte. This high operating voltage contributed to the considerably high energy density (a maximum of 30.4 Wh kg^{-1}), comparable, in order of magnitude, to redox-active electrolyte supercapacitors. On the other hand, the power density obtained at this high concentration was low (a maximum of 1.68 kW kg^{-1}) but increased as electrolyte concentration decreased – e.g. at 7 mol/kg, the reported energy and power densities were 25 Wh kg^{-1} and 2.1 kW kg^{-1}, respectively. Moreover, the authors reported that cyclability was also inversely correlated to electrolyte concentration – i.e., a very poor cyclability was reported for the highest concentration of electrolyte (31.5 mol/kg), whilst at 7 mol/kg 85% of capacitance retention was still observed after 2000 cycles. However, the higher concentration device still maintained a higher absolute capacitance when compared to lower concentration electrolytes. It should be noted though, that 2000 cycles is far from commercial standards.

5. Electrode materials

5.1. Carbon-based materials

5.1.1. Activated carbon

Activated carbon is currently the most common electrode material in commercial supercapacitors. It is usually obtained from the pyrolysis of carbon-rich organic precursors (e.g. coconut shell). The main advantages of this material are its large surface area, low cost and adaptability to mass production. However, since it presents a broad and unoptimized pore structure, a significant part of its surface area (30–60%) is not accessible to the electrolyte[8] and consequently does not contribute to capacitance [10,61,91,92]. An example where this problem is tackled is reported by Hwang et al. [93], where activated carbon electrodes underwent laser ablation to open microchannels which, in turn, shortened the diffusion distance and hence increased the capacitance and reduced the overall internal resistance of the electrodes. In this report, a high voltage of 2 V was possible because of the use of a redox-active electrolyte, ferrocyanide-ferricyanide in Na_2SO_4 aq. (which also contributed to an increased capacitance of the device). As such, a high energy density (18.9 Wh/kg) is simultaneously possible with a high power density (11.5 kW/kg).

It is not very common for a symmetric supercapacitor with activated carbon electrodes to present very high power and energy densities. When this happens, it is usually due to non-aqueous electrolytes (such as ionic liquids, as reported in [78]) and/or due to the presence of functional oxygen or nitrogen groups in the electrode surface that result in a considerable pseudocapacitive contribution [94,95]. Other examples of high power densities for carbon activated devices can be found in hybrid configurations (see Kim et al. [96] and Du et al. [97]).

Most commercial supercapacitors are symmetric devices with simple activated carbon electrodes and organic electrolytes. Therefore, one could tend to attribute the superior performances mentioned above to hybrid electrode materials and advanced electrolytes. However, lab-scale devices also made of symmetric carbon-based electrodes and organic electrolytes often outperform their commercial counterparts. This can in large part be clarified by the fact that different masses are considered in each situation: in commercial devices, the whole mass – including current collectors, electrolyte, separator, casing, etc. – is taken into consideration whereas in lab scale devices, only the active material mass of the electrode (which only accounts for about 30% of the total weight of the device [98]) is considered.

Typically, the active electrode material mass loadings of the lab and commercial devices are also distinct, < 5 mg/cm^2 and 10 mg/cm^2 , respectively [98]. The mass loading affects both the ESR and the gravimetric capacitance of the electrodes. For very low mass loadings (< 0.1 mg/cm^2), the results are usually unreliable[9]. For higher – but still low – mass loadings (between 0.1 and 1 mg/cm^2), gravimetric capacitance increases and as such energy density also increases whilst ESR increase is still not detrimental and thus power density remains high. When mass loading approaches commercial levels, the gravimetric performance tends to stabilize or even decrease (due to a decrease of the accessible area), and a detrimental increase in the ESR is also observed. The added mass thus does not present performance advantages. Commercial devices only use high mass loadings because of the necessary trade-off with the mass of rest of the device. In summary, literature reported performances of thousands of kW/kg or hundreds of Wh/kg obtained at very low mass loadings can be viewed as misguiding.

5.1.2. Activated carbon fibres

Activated Carbon Fibres (ACF) are threads – essentially composed by carbon atoms - with ca. 10 μm of diameter [99]), which were spun (often by electrospinning) and then subjected to a heat treatment[10] (under a controlled atmosphere – can be air, CO_2, Ar, etc.) in order to increase their surface area. These materials are suitable as supercapacitor electrodes due to the combination of their favourable mechanical properties (light weight and high tensile strength) with their high electrical conductivity [100], large specific surface areas and controllable pore size distributions [101]. These characteristics make them particularly attractive for portable and wearable electronics [102]. Main disadvantages are their more complex production as well as some long term stability problems that may arise due to their large surface area and to the presence of surface functional groups [10].

Due to their entangled structure, ACF provide a good matrix for

[8] specific surface areas can be as high as 3000 m^2/g but the usable areas fall in the range of 1000–2000 m^2/g [92].

[9] except when nanoparticles and thin films are involved; in these cases, it is very difficult to avoid very low mass loadings, but it does not necessarily mean that the results are unreliable – other criteria should be taken into consideration.

[10] Activation temperatures are usually between 800 °C and 900 °C.

embedding other active materials and therefore they can replace or significantly reduce the required amount of inactive binder polymers [103,104]. Thus, ACF are commonly found in hybrid devices, often associated to MnO_2 [102,105,106] – e.g. Fan et al. [105] reported an asymmetric device employing an Activated Carbon Nanofibre cathode and MnO_2/graphene composite anode with a gravimetric power density of 198 kW/kg which is significantly higher than conventional activated carbon devices.

Symmetric devices with non-composite ACF electrodes are also reported but present much lower performances. Yu and co-workers [107] produced ACF with large surface areas by chemically treating the CF surface to form ultrathin carbon sheets on the surface. Two ACF were then assembled into a fibre supercapacitor in PVA/H_3PO_4 gel electrolyte, which presented power and energy densities of 0.7 kW/kg and 70 mWh/kg, respectively[11]). A previous study, by Jiang et al. [108] had used a similar strategy to activate carbon cloth, but the supercapacitor (also symmetric) manufactured with the obtained ACF presented a slightly better performance (0.9 kW/kg and 324 mWh/kg [11]).

5.1.3. Carbon Nano Tubes (CNT)

Carbon Nano Tubes (CNT) are cylinders of one or more layers of graphene (Single-Walled Carbon Nano Tubes -SWCNT- and Multi-Walled Carbon Nano Tubes – MWCNT, respectively). CNT lengths range from < 100 nm to several cm. Diameters of SWCNT are typically between 0.8 and 2 nm whilst the diameters of MWCNT usually range from 5 to 20 nm [109]. They are also highly conductive [15].

CNTs can be synthesized through the catalytic decomposition of certain hydrocarbons [92,110]. Moreover, they can be grown on a conductive substrate as self-supporting films and as such do not require binding material. The result is a very efficient electronic contact to the substrate, unlike when a binder is used to provide mechanical stability [111,112].

CNT powders present a relatively low specific capacitance (20–80F/g) mainly attributed to their hydrophobic nature [110,113]. This can be mitigated by inducing additional pseudocapacitance via oxidative treatments that modify the surface texture and introduce additional surface functionalities [15,114].

Most of recent reports on CNT-based high-power supercapacitors have used CNT in a composite. This strategy has resulted in encouraging power and energy densities – e.g. Izadi-Najafabadi et al. [55] reported 990 kWh/kg for electrodes composed of a SWCNT/SWCNH composite. Here, the SWCNT served as a base-structure onto which SWCNH was deposited onto. The base SWNCT reduced the ESR and the resultant electrode morphology allowed for efficient electrolyte penetration and fast ion transport. Another example is the hierarchical structure of CNT covered by NiO nanosheets reported by Qiu et al [115]. These were used as the positive electrode, whilst the negative electrode was composed of defect-induced graphene sheets. The asymmetric devices achieved power and energy densities of 16 kW/kg and 16 Wh/kg, respectively.

An emerging trend are printable and/or flexible CNT-based devices. In 2016, Yu et al. reported an omnidirectionally stretchable supercapacitor composed of acid-treated CNT films covered with electrodeposited polyaniline (PAni) [116]. The power and areal energy densities were 9 kW/kg and 16 Wh/kg[12], respectively. In the same year, Ujjain and co-workers reported a printable and flexible device, based on functionalized MWCNT, with an energy density of 16 Wh/kg and a power density of 45 kW/kg [117]. These high values were attributed firstly, to the presence of functional groups that enhanced the electrode surface wettability (and hence ion mobility), and secondly, to the fact that no current collector was present (which led to a reduced ESR). Moreover, the ionic liquid electrolyte allowed for a wide operating voltage window. Another example of high-performance printable and flexible supercapacitor is reported by Kaempgen et al. [54]. Here, SWCNT were sprayed onto a flexible plastic substrate. The SWCNT networks served as both electrodes and charge collectors. The maximum reported maximum power density was 70 kW/kg whereas the energy density was only 6 Wh/kg – this, when using an organic electrolyte.

5.1.4. Carbide-Derived carbons (CDC)

Carbide-Derived Carbons (CDC) are carbon materials derived from carbide precursors (compounds made of carbon and another less electronegative element, such as a metal or metalloid). The methods used can be physical processes or chemical reactions [118]. Most CDCs are obtained through a chlorination process that causes the selective etching of the non-carbon element [119]. Some examples of carbide precursors are Al_4C_3, TiC, SiC, VC, Mo_2C, SiCN, $WTiC_2$, etc.

Depending on the carbide precursor, on the applied temperature and on the synthesis route, the carbon structure that remains can be, to name a few, amorphous, graphite, graphene, onion-like, open-fullerene like or nanodiamonds [119]. These materials have high specific surface areas and their pore-size distribution and their surface functional groups can be accurately controlled [120,121] making them especially attractive as electrode materials, despite the difficulties associated to the corrosiveness of the reactants involved [122].

Pohl et al. reported 200 kW/kg [123] symmetric supercapacitors where the carbon material is derived from TiC. Interestingly, in the same report TiC/CNT composite electrodes were shown not to enhance performance. Thomberg et al. reported vanadium carbide (VC) derived nanoporous carbon devices with a lower power density of 133 kW/kg [124]. Tee et al. [125] reported that CO_2 activated SiC-CDC electrodes resulted in a significant increase (more than 3 orders of magnitude) of the device's energy density, when compared to non-activated SiC-CDC: from ca. 1.6 mWh/kg to ca. 10 Wh/kg, both obtained at 2 kW/kg. The CO_2 activation increased the pore diameters, hence increasing the surface area actually accessible to the electrolyte ($EMImBF_4$) and this led to a dramatic energy gain.

It is common to find CDC in internal parallel hybrids (devices where each one of the electrodes is a composite containing CDC). One example can be found in the study by Zheng et al. [126], where calcium carbide (CaC_2) was combined with polyaniline (PAni) to form a composite material for supercapacitor electrodes (it should be noted that PTFE was also integrated as a binder as well as carbon black, to compensate the conductivity loss induced by the addition of PTFE). The obtained supercapacitors (whose electrolyte was an aqueous solution of H_2SO_4) achieved a reasonably high energy density (40 Wh/kg) but a moderate maximum power density (only 2 kW/kg) – higher energy densities were achieved, but at the expense of even lower power densities.

More recently, Tolosa et al. synthesized binder-free and free-standing electrospun niobium carbide/carbon nanofibre mats [127]. The binder and current collector absence contributed to a significant ESR reduction and, consequently, to the high value of maximum power density (30 kW/kg in an organic electrolyte). In these conditions, the energy density was only 7.6 Wh/kg. Higher values of energy density were achieved, but at the expense of a great reduction in power density (e.g. 19.5 Wh/kg at 0.01 kW/kg).

5.1.5. Graphene

Graphene can present itself in the form of "pure" graphene nanosheets (obtained through micromechanical exfoliation of graphite, reduction of graphene oxide, chemical exfoliation, electrochemical exfoliation [128] and by other methods as well – a comprehensive list can be found in Mohan et al. [129] and in Chen et al. [130]) or in graphene-

[11] Original values reported in mW/cm^3 and in mWh/cm^3. The gravimetric performances here presented were estimated according to the densities, explicit (1.8 g/cm^3 [107]) or implicitly (0.346 g/cm^3 [108]) presented in the articles.

[12] These values were originally presented in W/cm^2 and in Wh/cm^2; the results shown here were estimated according to the mass loading of 3.15 mg/cm^2, implicitly expressed in the article.

like carbon nanosheets (obtained through the carbonization of organic matters or biomasses with the assist of metal catalysts [119]). Graphene can also be in the form of an aerogel and in the form of graphene paper [131].

Graphene presents several interesting properties such as a large surface area, flexibility, good electrical conductivity, chemical and thermal stability, electrochemical stability and an abundant number of surface functional groups [132]. As such, it has been identified as a promising electrode material for supercapacitors and it is expected to be used in commercial devices as soon as its production becomes cost-effective on an industrial scale [133,134].

Besides its high cost, another disadvantage is the fact that graphene suffers from irreversible sheet restacking (forming graphite) resulting in a decrease in accessible surface area and hence in capacitance [135]. Yet, by combining graphene with conducting polymers [135] or with metal-oxide particles (which increase interlayer distance), sheet restacking (induced by Van der Waals forces [136]) is shown to be significantly reduced [137].

Panmand et al. [138] obtained perforated graphene from pyrolyzed Bougainvillea flowers and used this material in symmetric supercapacitors with a neutral aqueous electrolyte. The highest reported power was 7.3 kW/kg at a corresponding energy density of 14.6 Wh/kg. Recently Banda et al. [139] obtained a lower energy density (4.3 Wh/kg) but also a significantly higher power density (38 kW/kg) for symmetric graphene based devices with an alkaline electrolyte. The high power density is attributed to the highly porous nature of the graphene hydrogel – a solid jelly like material, obtained by the addition of a diamine (hydrazine, in this case) to a solution of graphene oxide, followed by sonication, heat treatment and air drying steps. Also in 2017, Yang et al. [140] achieved similar power densities (41 kW/kg) but with a significant increase in energy density (148.8 Wh/kg) for a symmetric highly porous graphene based device. The higher energy density is attributed to the large operational window afforded by the ionic liquid. Although the energy density decreased to 31.4 Wh/kg for organic electrolyte devices, it still presents a ca. 7-fold increase when compared to Banda et al.'s report.

Associating metal oxides with graphene can have the twofold benefit of preventing graphene restacking along with the addition of pseudocapacitance. One example is where manganese oxide and graphene oxide are combined, as reported by Kumar et al. [141]. The power density was not noteworthy (7.1 kW/kg), however, an energy density of 58 Wh/kg was demonstrated (for an organic electrolyte device).

Graphene with conducting polymer combinations have also shown promise: when combined, graphene can provide mechanical support and enhance the electrical conductivity while the polymers prevent the graphene sheets from restacking and add a pseudocapacitive contribution [61].

5.1.6. Carbon aerogels

Carbon aerogels are highly porous carbonaceous materials whose internal structure is monolithic and characterized by a regular pore structure. These materials are good candidates for supercapacitor electrodes due to their high electrical conductivity, high mechanical stability and also due to their high mesoporosity (since mesopores facilitate the ion transport and hence enable a high capacitance retention even at high current densities).

Hao et al. [142] derived an hierarchical porous carbon aerogel from bagasse through activation at high temperatures (ranging from 700 to 900 °C) with KOH. Symmetric devices with a KOH-PVA gel electrolyte were shown to achieve 10 kW/kg and 11 Wh/kg of power and energy densities respectively. More recently, Lin et al. [143] derived powdery carbon aerogels from poly(styrene-co-divinylbenzene) (PSDVB) nanoparticles. Symmetric devices with an organic solvent electrolyte achieved a lower power density (4 kW/kg) – perhaps due to the larger size of the solvated ions (although the aforementioned electrolyte was solid, it had an aqueous solution "trapped" within the polymer and aqueous electrolytes have a much higher mobility than their organic counterparts) – but it also achieved a higher energy density (32 Wh/kg) – probably explained by the wider voltage window of the electrolyte.

5.2. Transition metals

5.2.1. Transition metal oxides (TMO)

Transition metal oxides (TMO) have been identified as suitable pseudocapacitive materials. TMO offer a variety of oxidation states and can undergo fast, coupled and reversible redox reactions at overlapping potentials. This overlap is the cause for the almost rectangular CVs, characteristic of TMO and indicative of their pseudocapacitive behaviour [20]. For these surface redox reactions (responsible for the increased energy densities) to occur at high rates, it is important that these materials possess numerous active sites [144]. Moreover, to still ensure high power density, these materials should not present a high resistivity. Finally, in order to have an acceptable cyclability, the selected transition metal oxides should also have a high chemical, mechanical and thermodynamic stability. Ruthenium oxide and manganese oxide are the TMO which better meet these requirements and, as such, are the most commonly used in supercapacitors.

5.2.1.1. Ruthenium oxide (RuO_2). Ruthenium Oxide (RuO_2) is a transition metal oxide that undergoes electron transfer reactions upon the electrochemical adsorption of protons onto its surface [20]. It can exist in two different phases: a crystal phase and an amorphous hydrous phase ($RuO_2{\cdot}xH_2O$). Nanostructured RuO_2 can be synthesized via several methods including hydrothermal synthesis, template, microwave, electrodeposition, solid-state method and oxidative precipitation. Its nanostructure (either as a nanoparticle, nanofibre or nanorod) is highly affected by the annealing. For example, high annealing temperatures (300–800 °C) lead to the formation of ruthenium oxide's crystalline phases and to a decrease in the water content of the material, which consequently changes the number of active reaction sites, as well as the electron and proton conductivity [119].

RuO_2 is very attractive as an active electrode material for supercapacitors due to its high specific capacitance (mainly pseudocapacitance), good thermal stability, highly reversible redox reactions in a wide potential range, high rate capability and long cycling life [145]. Its main disadvantage is its scarcity and consequently prohibitive cost. For this reason, purely RuO_2 electrode devices are commercially uncommon.

The high performance of RuO_2 is exemplified by Hu et al. [146], who reported a maximum power density of 4320 kW/kg. This was for hydrous RuO_2 nanotubular arrayed electrodes in H_2SO_4. The success is attributed to its morphology which permits direct and therefore efficient ion diffusion. A caveat is that the mass loading was very low (only 0.2 mg/cm^2). Moreover, this result was obtained in a three-electrode setup; not for a complete device. A symmetric device with the same electrolyte would theoretically present approximately a quarter of the energy density, only 1.9 Wh kg^{-1}, and a quarter of the power density, 1080 kW/kg.

Significantly lower power densities are reported when a nanotubular structure is not employed. Xia et al. reported 10 kW/kg (and 15 Wh/kg of energy density, correspondingly) for a symmetric aqueous electrolyte device employing nanocrystalline hydrous RuO_2 [147]. Yet, it should be noted that 10 kW/kg was not necessarily the maximum achievable power density of the device; it simply corresponded to the power density obtained at the maximum current density used in the tests (12.5 A/g) – perhaps at higher current densities, higher power densities (and lower energy densities) would be obtained.

Due to its prohibitive cost, most of the RuO_2 used in supercapacitors is in the form of nanoparticles, combined with other active materials, such as MnO_2 [148] and non-active materials, such as nanoporous gold

[149] (which simultaneously acts as an enhanced mechanical support for the metal oxide and as a current collector).

5.2.1.2. Manganese oxide (MnO_2). Manganese oxide (MnO_2) has a high theoretical capacitance, similarly to RuO_2. It is usually prepared through a hydrothermal synthesis and, depending on the temperature and dwell time of the process, it can present several morphologies [150]. It is possible to obtain highly desirable tailored nanostructures to enhance capacitance and ionic conductivity. MnO_2 is significantly more economical than RuO_2. However, conductivity is low (10^{-5}–10^{-6} S/cm [151]) as is its chemical stability in acidic media [119]. An example where conductivity was enhanced can be found in Kang et al. [152], where the material was doped with Au atoms, which subsequently enhanced the specific capacitance of the films.

Reports of supercapacitors exclusively made of manganese oxide are very uncommon, namely because of its low conductivity. Suitable performances are reported when MnO_2 is associated with carbon-based materials (e.g. graphene [153], CNT or activated carbon [52]). The result is an enhanced electrode mechanical stability and conductivity. However, MnO_2 on its own is an interesting option for low power, low energy applications such as microelectronics. Wang et al. [154], reported micro-supercapacitor exclusively made of MnO_2 nanosheets deposited on a SiO_2 substrate. The planar device employing an aqueous $NaNO_3$ electrolyte displayed an areal power and energy densities of 217 mW/cm^2 and 3 mWh/cm^2.

5.2.2. Transition metal sulphides (TMS)

Transition metal sulphides (TMS) are also suitable electrode materials. Due to their facilitated pathway for electron transport [155], TMS usually present higher conductivities and higher capacitances than their oxide and hydroxide counterparts. Yet, they suffer from the same cycling stability problems as metal oxides. As such, instead of being used as single electrode materials, the current research trend is to hybridize TMS with graphene.

Several transition metals can be used in these compounds, but the TMS most usually found in literature-reported supercapacitors are cobalt sulphide, nickel sulphide, molybdenum sulphide and sometimes binary (or even ternary) sulphides, such as nickel–cobalt sulphide [156].

Gigot et al. [157] obtained a hybrid aerogel, composed of MoS sheets of two different phases intercalated with rGO layers. The symmetric supercapacitor built with this hydrothermally co-synthesized composite was able to provide 12.6 Wh/kg while maintaining a power density of 3.2 kW/kg. More importantly, the as-fabricated device showed a capacitance retention of nearly 100% after 50000, which is very unusual for non-carbon materials. This outstanding cyclability is, according to the authors, due to the enhanced conductivity and mechanical stability provided by graphene, combined with the redox reactions undergone by the MoS sheets.

Xu and Lu [158] obtained a cobalt sulphide-reduced graphene oxide composite which was then used as active electrode material in a symmetric supercapacitor. The device, despite having an aqueous electrolyte (KOH), achieved a noteworthy performance: an energy density of 13.6 Wh/kg at a high power density of 24.5 kW/kg. Moreover, a capacitance retention of 90% after 5000 cycles was observed. The high energy density can be attributed to the reversible redox reactions undergone by the CoS, whilst the ability to charge and discharge many times at a fast rate is mainly due to the high conductivity and mechanical stability of rGO. Also of interest, the composite material was obtained via a one-step synthesis, through a hydrothermal method.

Jothi et al. [159] also synthesized a TMS through a simple strategy: by using the triblock copolymer poloxamer 123 as a structure-directing agent, the authors obtained a nanoporous and highly controlled two-dimensional nickel sulphide. This material was then hybridized with 40% of rGO sheets and the resulting composite served as a positive electrode in an asymmetric device (ZIF-8-derived carbon was used as the negative electrode). The supercapacitor achieved an energy density of 13.4 Wh/kg at a power density of 10.3 kW/kg.

Other reports claim higher electrochemical performances with binary sulphides containing both nickel and cobalt. For instance, Yang et al. [160] obtained Ni-Co-S nanoparticles enriched with electroactive edge-sites and anchored on graphene frameworks. This material was then used as the positive electrode of a supercapacitor (the negative electrode was made of porous carbon nanosheets). The as-fabricated device showed an excellent electrochemical performance, by providing more than 28 Wh/kg at a high power density of 22 kW/kg. The cyclability was also encouraging: the asymmetric supercapacitor retained 90% of its initial capacitance after 8000 cycles. Xiao et al. [161] obtained equally interesting results for nickel–cobalt-sulphide nanoparticles on graphene nanosheets. The asymmetric device using this composite as a positive electrode and activated carbon as the negative electrode reached 37.7 Wh/kg at 17 kW/kg. Moreover, it showed an impressive capacitance retention of 96% after 5000 cycles.

5.3. Conducting polymers

Due to their pseudocapacitive behaviour, conducting polymers demonstrate significantly higher energy densities (2–5 times [162]), when compared to carbon-based materials. Moreover, it is well known that they can be directly electrodeposited on the current collector (enabling lighter binder free electrodes) and that their structure and film thickness can be tailored by tuning the parameters of the electrodeposition. Finally, because of the growing interest in flexible devices, there is added interest in conducting polymers. Despite their flexibility, it is also well known that repeated shrinking and swelling (upon charge–discharge) induces degradation, which ultimately reduces their cycle-life. Indeed, their capacitance retention is much lower than the one achieved by carbon-based materials. Besides their low cyclability (usually no more than 2000 cycles), their power density is compromised by their slower response (their typical power density is around 4 times smaller), when compared to carbon-based materials. Therefore, instead of being used as single electrode materials, conducting polymers tend to be used as a composite material, often combined with carbon-based materials and/or metal oxides, which can improve their mechanical stability and their power density [163].

5.3.1. Polypyrrole (PPy)

The conducting polymer Polypyrrole (PPy) is an attractive pseudocapacitive material due to its mechanical flexibility, tuneable electrical conductivity, high capacitance (associated to its redox properties), low cost, low environmental impact and ease of manufacture. Synthesis routes are chemical (through the oxidation of the pyrrole monomer) or electrochemical polymerization. The latter enables direct growth on the current collector and hence does not require binders for mechanical stability. As such, electrical conductivity is also higher. Moreover, electrochemical polymerization allows the fine control of deposited mass and, therefore, thickness [164].

As already mentioned, a common drawback with conducting polymers is their poor cyclability, to which PPy is not immune. This is due to the continuous swelling (during oxidation) and shrinking (during reduction) [165]. This can be minimized by growing/coating PPy on a flexible substrate (e.g. graphene nanosheets or carbon cloth [166]) or by adding a doping anion [164]. Flexible substrates permit volume changes without inducing large local stresses. Anion doping - such as β–naphthalene sulfonate anions (NS-) – can effectively suppress the counterion drain effect, since these dopants can remain in the backbone of PPy chain and consequently prevent the degradation of the polymer's structure. By using these strategies, Song et al. [167] reported PPy-based devices with 97% capacitance retention after 10 000 cycles.

Meng and Ding [168] also explored the association between PPy and a flexible – yet robust – substrate. The authors coated 100 nm-thick nanoporous gold (NPG) films with an 8 nm-thick PPy film and

assembled the as-fabricated electrodes into a symmetric all-solid-state device, with a $HClO_4$ -PVA gel electrolyte. Considering exclusively the mass of the active material (PPy), the authors claim a maximum power density of 296 kW/kg and a maximum energy density of 27 Wh/kg. Here the current collector also provided mechanical stability to the active layer. Cyclability was comparatively low, with a 78% of capacitance retention after 900 cycles, but it is still considered reasonably high for devices employing PPy.

Another noteworthy high performance of a PPy based device was reported by Zhang et al. [169]. Highly orientated horn-like PPy arrays were electrochemically grown and used to form solid state symmetric devices employing H_3PO_4-PVA gel electrolyte. The specific power and energy densities are lower, 1.2 kW/kg and 9 Wh/kg, respectively. However, film thickness is significantly higher – at ca. 10 μm – as is the cyclability, with a capacitance retention of 88% after 10 000 cycles.

5.3.2. Poly(3,4-ethylenedioxythiophene) (PEDOT)

Similarly to PPy, PEDOT also demonstrates good electrical conductivity (when oxidized; the reduced form has poor conductivity). Moreover, p or n doping are both possible, low oxidation potential with a wide voltage window (1.2–1.5 V) and thermal and chemical stability are high [170]. However, cyclability is low. Strategies to circumvent this problem are the same as for other polymers, namely forming composites to enhance the mechanical stability (e.g. PEDOT-CNT or PEDOT-graphene composites [171–173]).

In terms of performance, examples of noteworthy reports are that by Liu et al. [174] and Rajesh et al. [175] which employed nanotubular PEDOT structures. Reported power densities were 25 kW/kg and 40 kW/kg respectively and energy densities were 5.6 Wh/kg and 4.4 Wh/kg respectively. The directionality of the tubes allows for rapid ionic transport whilst the nature of the nanotube wall enables the rapid redox processes because of the short diffusion distance to the counterions. In the Liu et al. [174] report no indication was given as to capacitance retention upon cycling, whilst Rajesh et al. [175] reported the noteworthy 86% capacitance retention after 12 000 cycles. The direct growth of the nanotubular structure on flexible 3D carbon fibre cloth by facile in-situ hydrothermal polymerization permits the devices to have a low ESR and also permits the PEDOT structure to expand and contract freely thus enhancing the capacitance retention. Also the technique and materials are amenable for upscaling unlike the case of Liu et al. [174], where Au is employed in the templated electrochemical film growth process.

5.3.3. Polyaniline (PAni)

Polyaniline (PAni) is a conducting polymer with several oxidation states thus facilitating the tuning of its pseudocapacitive behaviour [176]. It is also a flexible polymer and can be grown directly onto current collecting substrates. Another key feature of this material is the fact that polyaniline-based supercapacitors have been reported to have low self-discharge [177].

PAni conductivity increases significantly when doped in strong inorganic acidic media (e.g. HCl) [178]. Moreover, the resulting morphology is non-optimal and therefore accounts for its low cyclability and for a significant capacitance drop at increased current densities. Weak organic acid doping (e.g. with phytic acid) results in better morphological features, but also in reduced conductivities. Gawli et al. [179] successfully tackled this problem by co-doping PAni with these two acids. The resulting three-dimensional structure showed a significant capacitance retention at a broad range of current densities and an acceptable cyclability at a very high current density (500 cycles at 40 A/g). After the doping step, PAni also performs better in acid electrolytes, which causes constraints with respect to the materials that can be employed in the device and packaging. A way to circumvent this problem is by the self-doping mechanism which has allowed for the reporting of high performance devices in neutral electrolytes [180].

Ghenaatian et al. [181] used self-doped PAni nanofibres as electrodes in a symmetric supercapacitor with an acid electrolyte (10^{-3} M HCl and 1 M KCl) and obtained a power density of 3.5 kW/kg and an energy density of 6 Wh/kg. However, cyclability was low with only 50% of capacitance retention after 1000 cycles.

A significantly higher 70 Wh/kg energy density and 7 kW/kg was reported by Prasad et al.[182]. The higher energy density can be attributed to the wider operating voltage of the organogel electrolyte (gel polymer soaked in a solution of $LiClO_4$ in propylene carbonate). However, cyclability was still far from the one required for promising devices (only 91% of capacitance retention after 1000 cycles). Li et al. [183] managed to obtain a much higher capacitance retention (86% after 17,000 cycles) for a symmetric all-hydrogel-state fibrous supercapacitor. The combination of PAni hydrogels and reduced graphene oxide (RGO) rendered the fibres enhanced mechanical properties which translated into a higher cyclability.

5.4. Other materials

After the advent of graphene, alternative two-dimensional materials started to be investigated for ultrathin flexible devices. Although some interesting results were obtained for transition metal phosphates (e.g. 2-D vanadyl phosphate was successfully used as an electrode material for a pseudocapacitor [184]), Metal Organic Frameworks (MOFs), Covalent Organic Frameworks (COFs) and MXenes seem to represent the main research trends in 2-D materials for supercapacitors.

5.4.1. Metal-Organic Frameworks (MOFs)

Metal-Organic Frameworks (MOFs) are porous coordination polymers (i.e. metal cation centres linked by organic ligands in an organized 1-D, 2-D or 3-D architecture). These materials simultaneously present a light, rigid and flexible structure (which promotes an increased cyclability), with a large surface area and a highly tuneable porosity. Moreover, if redox metal centres are incorporated, MOFs can display, to a certain degree, a pseudocapacitive behaviour.

Zhang et al. [185] recently reported an asymmetric device composed of synthesized 2-D layered Ni-MOF electrode and a carbon activated carbon electrode. High specific capacitances were observed, 161F/g at 2 A/g. By doping the Ni-MOF with Zn, Yang et al. [186] demonstrated higher capacitance at even higher current densities, namely 854F/g at 10 A/g. The dopant prevents the collapse of the crystal lattice and also enlarges the interlayer distance, hence improving the diffusion of the electrolyte ions within the electrode. Zirconium-based MOFs (without doping) were also shown to achieve a high specific capacitance (726F/g [187]).

Comparatively, MOFs still yield low performance because of their low conductivity. Despite these good results, the majority of MOFs yield moderately low performances due to their reduced electronic conductivity. To overcome this limitation, composites with carbon have also been explored and managed to improve the performance [188]. MOFs have the potential to be low-cost, because of the materials involved. However, there is still uncertainty as to yields because the synthesis is complex [189]. Nevertheless, there is significant interest in finding routes for upscaling. An excellent review by Rubio-Martinez et al. [189] focuses on this topic and shows that there are also a number of significant commercial applications outside electrochemical energy storage [190] (e.g. micro-adsorbents for food conservation, gas storage, etc.).

5.4.2. Covalent-Organic Frameworks (COFs)

Covalent Organic Frameworks (COFs) are porous crystalline polymers where the organic building blocks are linked through strong covalent bonds, forming a 2-D or 3-D structure [191]. These typically have a high surface area, tuneable pore sizes and very flexible molecular designs [188], making them attractive electrode materials. Pseudocapacitive behaviour is observed when combined with redox active species (e.g. anthraquinone, pyridine, etc.) and conducting

polymers.

5.4.3. Mxenes

MXenes are 2-D transition metal carbides and carbonitrides (such as Nb_2C, Ti_3C_2, Ta_4C_3, etc.). These tend to have high conductivities, good mechanical properties, and high hydrophilicity, making these good electrode materials. $Ti_3C_2T_x$ in particular was shown to have a high volumetric capacitance in aqueous electrolytes, 245F/g [192] (smaller capacitances were obtained in organic electrolytes [193]).

However, these materials often suffer from re-stacking of the MXene flakes, which reduces their accessible surface area and, consequently, their capacitance. Therefore, combining MXenes with interlayer spacers – such as hydrazine [194], polypyrrole [195] or PVA [196] – was shown to significantly improve the performance of Ti_3C_2-based MXenes by increasing their flexibility, their capacitance and also their cyclability.

6. Literature-reported performances

This section presents a collection of recent literature-reported performances in terms of gravimetric energy and power densities. Despite the complex and multivariate nature of the factors influencing these two indicators, it is clear that the choice of the electrolyte and electrode materials has a significant impact on the performance of the as-fabricated devices. Some materials are more suitable than others and some material combinations work better than others. For each type of material combination, the best performing devices (with available information about the energy and power densities) were included.

Examples of simple symmetric supercapacitors were presented in the previous sections. As the current literature largely favours hybrid architectures, the following tables are mainly devoted to ISH, IPH and DH devices (see section 2). Nevertheless, since simple symmetric supercapacitors can be considered a particular case of ISH and IPH, some table-entries also include this type of configuration.

In total, there are three tables: Tables 1a and 1b are for devices using aqueous electrolytes (gel polymers with aqueous solutions -e.g. H_2SO_4 in PVA – are also included here), Table 2 is for organic electrolytes and Table 3 is for ionic liquids. Each table is divided in three parts: the upper rows are devoted to ISH, the middle rows are for IPH and the lower rows are for DH. The first column of each table expresses the type of material combination. For simplicity, and given the numerous active electrode materials (and, consequently, the many possible associations), the types of material combinations were divided into four categories: carbonaceous materials (“C”), metal oxides/hydroxides (“MO”), metal sulphides (“MS”), conducting polymers (“CP”) and other materials - COFs, MOFs, MXenes, etc. – (“Other”). The third and fourth columns, respectively show the specific powers of the devices and their corresponding specific energies. Whenever possible, the energy and power densities used were from the same point of the Ragone plot (i.e. were obtained at the same current density). When Ragone plots were not available, the energy and power densities correspond to different “points of operation”: point of maximum power and minimum energy and vice-versa. These occasional cases are highlighted in the “Additional remarks” column. In some instances, the gravimetric performance was estimated from the stated volumetric performance and from the explicit (or implicit) density of the active electrode material (this is also indicated in the last column of the table, together with other useful data).

The fact that Tables 1a and 1b has the largest number of rows is a proxy of an important research trend: supercapacitors with aqueous electrolytes have lately received a lot of attention. And, among these, double hybrids (most of the times having one or both electrodes made of carbon–metal oxide composites) are the most abundant ones. Exotic and highly complex electrode structures are also prevalent: “nanowires” and “nanotubes” are terms often found in the columns describing the electrodes.

Fig. 3 shows the performances of the devices mentioned in Table 1a, Table 1b, Table 2 and Table 3, grouped by the type of electrode materials and Fig. 4 shows the same information, but in this case the devices are, grouped by the type of electrolyte. In both Ragone plots, the values of power and energy densities that did not correspond to the same point ([206;226]) were not included.

The first conclusion that can be drawn out of the plots shown in Fig. 3 and in Fig. 4 is that no trend is visible in none of the groups. This is less surprising for the first of these plots, since there are fewer data points available for each type of material combination (the most common hybridizations are between carbon-based materials and metal oxides – the “C-MO” type; some of the other groups only have one or two elements, which is clearly insufficient to conclude anything). Still, even for the “C-MO” group, although it appears to have a slightly larger concentration of points around the 20Wh/kg (which could suggest that the energy density of these kind of devices does not suffer as much with increased rates of discharge), the dispersion of results is too large to extract any solid inferences.

Besides the obvious lack of data points in each group, the absence of a trend could also be linked to an unoptimized categorization. For instance, having an activated carbon electrode is not the same as having graphene or carbon nanotubes. Although all of these are carbonaceous materials, their structure and pore size distributions are fairly different, which can lead to very different accessible surface areas and, consequently, to very different capacitances. One could then argue that it would be more adequate to group the electrode materials according to their accessible surface areas, since this – along with the existence/inexistence of pseudocapacitance – should, theoretically, be the best predictors for capacitance. Yet, it is worth stressing that the accessible surface area is also largely dependent on the electrolyte. In fact, rigorously quantifying it for a certain device is taxing.

Moreover, even if these criteria would decrease the dispersion of results within each group, the conclusions would then be trivial: the devices having electrodes with a larger accessible surface area and/or pseudocapacitive materials tend to present a higher capacitance and that leads to higher energy densities. Notwithstanding, this is only true when considering devices with the same electrolyte. Since energy density (as well as power density) largely depends on the voltage window, the type of electrolyte cannot be ignored. Indeed, another probable explanation for the absence of trends in both Ragone plots is the fact that neither the type of electrode materials nor the type of electrolyte alone is enough to explain performance. The energy and power densities of a certain device result from the combined features of these two elements.

Yet, since the performance is proportional to the square of the voltage window and since there are more data points available for each group of Fig. 4, one could perhaps expect a slightly larger concentration of aqueous electrolyte devices (typical $\Delta V \approx 1$ V) in the lower left area of the plot and a slightly larger concentration of devices having an ionic liquid (typical $\Delta V \approx 4$ V) in the upper right area of the plot. However, this is not the case and, in fact, one of the best performing devices has an aqueous electrolyte. This raises another worth-mentioning caveat: most of the results recently published in the literature correspond to successes and, therefore, to devices that stand out from their counterparts. Hence, since effort has recently been put into widening the voltage window of aqueous electrolytes, it is not surprising that some of the outstanding results presented here already reflect these efforts and therefore contradict the expected behavior.

The aim of this material-based categorization was to provide a simple and straightforward comparison between different types of electrolytes and different combinations of electrode materials. Due to the relatively small amount of data and to the complexity of the factors influencing the performance, it was not possible to obtain any visible trend among the groups. Notwithstanding, this exercise enabled two observations:

Table 1a
Performances of literature-reported devices with aqueous electrolytes (ISH and IPH).

Type	References	Power density, kW/kg	Energy density, Wh/kg	Positive electrode	Negative electrode	Electrolyte	Additional Remarks
C//C	Hwang et al., 2017 [93]	11.5	18.9	activated carbon	activated carbon	H_2SO_4 with $Fe(CN)_6^{3-}$ /$Fe(CN)_6^{4-}$	electrodes were treated with a CO_2 laser
C//MO	Maitra et al., 2017 [197]	3.2	15.8	Zn − Fe − Co ternary oxide (ZICO) nanowires	N-doped graphene nanosheets	PVA − KOH gel	current collectors: nickel foam; encapsulated in polydimethylsiloxane
C//CP	Dubal et al., 2016 [198]	3.2	10	PPy nanotubes	N-doped CNTs	H_2SO_4	–
C//Other	Couly et al., 2018 [199]	0.7	2.7	reduced graphene oxide	$Ti_3C_2T_x$-MXene	PVA − H_2SO_4 gel	estimated from the volumetric energy and power densities of the article's Ragone plot, from the packing density of the MXene − 4 g/cm^3- and from the density of reduced graphene oxide − 2 g/cm^3 [1] - (average density of 3 g/cm^3)
MO//MO	Chen et al., 2014 [149]	90	70	$Co(OH)_2$ on nanoporous gold	RuO_2 on nanoporous gold	NaOH	78% of capacitance retention after 3 000 cycles
CP//CP	Li et al., 2016 [200]	16.2	3.2	PEDOT:PSS film	PEDOT:PSS film	PVA/H_3PO_4 gel	estimated from the volumetric energy and power densities mentioned in the article and from the stated density of the polymer − 1 g/cm^3
Other//Other	Xia et al., 2017 [201]	0.3	1.2	Ni-dMXNC	$Ti_3C_2T_x$ MXene	KOH	estimated from the volumetric energy and power densities mentioned in the article and from the total density of the active materials − 4,3 g/cm^3 - which was estimated according to the information given in the article
MO//C	Chen and Xue, 2016 [202]	2.5	16.2	$V_2O_3(OH)_3$ and $VO_2{\cdot}H_2O$	activated carbon	KOH	77% of capacitance retention after 1000 cycles
MS-C//MS-C	Xu and Lu, 2015 [158]	24.5	13.6	CoS/rGO		KOH	90% of capacitance retention after 5000 cycles; electrodes also contained 10% of carbon black ad 10% of nafion
MS-C//MS-C	Jia et al., 2017 [203]	1	10.6	MoS_2 @ graphene nanobelts		KOH	97% of capacitance retention after 1000 cycles
MS-C//MS-C	Gigot et al., 2016 [157]	3.2	12.6	co-synthesized rGO-MoS_2		NaCl	nearly 100% of capacitance retention after 50,000 cycles
C–C//C–C	Xie et al., 2016 [204]	4.7	12.2	Core-shell N-doped active carbon fibre and graphene		KOH	retention rate of 71%
C-MO//C-MO	Wen et al., 2017 [103]	17.4	4	carbon fibre sheets/MnO_2		Na_2SO_4	self-supported and binder-free electrodes; carbon fibres were obtained from disposable bamboo chopsticks
C-CP//C-CP	He et al., 2018 [172]	10.2	8	flexible free-standing 3D CNTs/PEDOT sponge		H_2SO_4 in PVA gel	no conductive additives nor binders were used
C-Other//C-Other	Yan et al.,2017 [205]	24	3.3	MXene nanosheets and reduced graphene oxide		H_2SO_4	values refer to 5% content of graphene; 61% of capacitance retention at 1 V/s
MO-MO//MO-MO	Sun et al., 2013 [206]	72	9	MnO_2 nanowires supported on hollow Ni dendrites		Na_2SO_4	maximum values (not at the same point)
MO-Other//MO-Other	Zhang et al., 2016 [207]	11.5	210	MnO_2@manganese hexacyanoferrate hydrate nanocubes		KOH in PVA gel	95% of capacitance retention after 10 000 cycles, at 10A/g
CP-Other//CP-Other	Peng et al., 2016 [208]	0.4	35	PPy/nickel sulphide/bacterial cellulose		NaCl	–
(…)	(…)	(…)	(…)	(…)		(…)	(…)

Table 1b
1- Performances of literature-reported devices with aqueous electrolytes – continuation (DH).

Type	References	Power density, kW/kg	Energy density, Wh/kg	Positive electrode	Negative electrode	Electrolyte	Additional Remarks
(…)	(…)	(…)	(…)	(…)	(…)	(…)	(…)
C-MO//C	Fan et al., 2011 [105]	198	8	graphene and MnO_2	activated carbon nanofibres	Na_2SO_4	–
C-MO//C	Qiu et al., 2017 [115]	16	16.2	hierarchical CNT@NiO core–shell nanosheet	graphene	KOH	–
C-MO//C	Ahuja et al., 2017 [148]	31.6	2	MnO_2 and RuO_2 @GNR	GNR	Na_2SO_4	point of maximum power density (and minimum energy density)
C-MO//C	Chen et al. [209]	5.2	13	activated carbon	$LiMn_2O_4$ and carbon particles (Super P) composite	Li_2SO_4	85% of capacitance retention after 4 500 cycles
C-MO//C	Khomenko et al., 2006 [52]	123	21	MnO_2 - CNT	activated carbon	KNO_3	PTFE was used as a binder
CP-MO//C	Zhou et al., 2013 [210]	5.5	11.8	PPy on CoO nanowire arrays	activated carbon	NaOH	carbon additive- and binder-free
CP-C//C	Hashemi et al., 2018 [211]	15.9	12.6	PAni and Functionalized Carbon Cloth (FCC)	activated carbon and FCC	H_2SO_4-PVA, redox additive, acetic acid	the negative electrode contained PTFE
MO_1-MO_2//C-MO_3	Wang et al., 2016 [212]	8	9.1	$CuCo_2O_4$-CuO nanowires	RGO-Fe_2O_3	KOH	–
C-CP//C	Yu et al., 2016 [213]	12.6	14	Hierarchically porous carbon/PAni	Hierarchically porous carbon	Na_2SO_4	92% capacitance retention after 5 000 cycles
MS-MO//C	Niu et al., 2016 [214]	5	11	$NiCo_2S_4$ deposited on Ni_3V_2O	activated carbon	KOH	94% of capacitance retention after 5 000 cycles
MO_1-C//MO_2-C	Liang et al., 2018 [215]	12.3	29	$Ni(OH)_2$ @ CC	$Fe(OH)_3$ @ CC	KOH	41% of capacitance retention after 10 000 cycles
MS-C//C	Chen et al., 2017 [216]	6.6	9.2	CoS_2 @ reduced graphene oxide (rGO) nanofibres	activated carbon	KOH	95% of capacitance retention after 2 000 cycles
MS//MS-C	Patil et al., 2017 [217]	0.4	1.1	Co_3S_4	Co_3S_4-rGO	PVA-KOH	90% of capacitance retention after 5 000 cycles
C//MS-C	Lin et al., 2015 [218]	7.2	13.4	reduced graphene oxide hydrogel	Co_9S_8 @3D graphene	KOH	86% of capacitance retention after 6 000 cycles
MS-C//C	Jothi et al., 2016 [159]	10.3	13.4	nanoporous nickel sulphide flakes @ rGO sheets	ZIF-8-derived carbon	KOH	–
MS-C//C	Annamalai et al., 2017 [219]	7.1	45.3	$NiCo_2S_4$@rGO	Graphene/single wall carbon nanohorns	KOH	–
MS-C//C	Beka et al., 2017 [220]	2.5	29.9	$NiCo_2S_4$ nanotube core and a $Co_xNi_{(3-x)}$ S_2 shell @ graphene on Ni foam	rGO	KOH	93% of capacitance retention after 5 000 cycles
MS-C//C	Yang et al., 2016 [160]	22.1	28.4	Ni–Co–S nanoparticles on graphene	porous carbon nanosheets	KOH	90% of capacitance retention after 8 000 cycles
MS-C//C	Xiao et al., 2015 [161]	17	37.7	$NiCo_2S_4$ @ graphene	activated carbon	KOH	96% of capacitance retention after 5 000 cycles
MS-C//C	Zhou et al., 2017 [221]	4	2.1	MoS_2@3D graphene	activated carbon	KOH	110% of capacitance retention after 4 000 cycles

Table 2
Performances of literature-reported devices with organic electrolytes.

Type	References	Power density, kW/kg	Energy density, Wh/kg	Positive electrode	Negative electrode	Electrolyte	Additional Remarks
C//C	Ahmed et al., 2018 [70]	57	18	activated carbon	activated carbon	$LiClO_4$ in EC/PC	PVDF-HFP was used as a binder and acetylene black as a conductive additive
MO//CP	Du Pasquier et al., 2002 [222]	0,56	6,1	PFPT	lithium titanate	1 M $LiPF_6$ in 1 EC-1 DMC	–
CP//CP	Liu et al., 2008 [174]	25	5,6	PEDOT nanotubes	PEDOT nanotubes	Et_4NBF_4 in propylene carbonate	–
Other//Other	Acerce et al., 2015 [223]	3,16	3,16	1 T MoS_2 electrodes	1 T MoS_2 electrodes	EMIM BF_4 in acetonitrile	estimated from the volumetric energy and power densities mentioned in the article and from the total density of the active materials − 10 g/cm^3 - which was estimated according to the information given in the article
C–C//C–C	Zheng et al., 2014 [224]	1,1	6	graphene/activated carbon nanosheet		Et_4NBF_4/PC	point of maximum power density (higher energy densities can be extracted but at lower power densities)
C-MO//C-MO	KM et al., 2017 [141]	7,1	58	nanocomposite of MnO_2 and reduced graphene oxide		tetraethylammonium tetrafluoroborate in acetonitrile	PVDF was used as a binder and carbon black as a conductive additive
C-CP//C-CP	Niu et al., 2012 [225]	62,5	131	SWCNT/PANI		$LiClO_4$ in a mixture of ethylene carbonate, diethyl carbonate, and dimethylene carbonate	maximum energy and power densities (not obtained at the same point); the electrodes acted as current collectors
CP-MO-C//C	Zou et al., 2010 [226]	0,2	61	PANI/MnO_2/ activated carbon	activated carbon	$LiClO_4$ in acetonitrile	–
C-MO//C	Chen et al., 2011 [227]	0,63	30	CNT/V_2O_5 nanowires	activated carbon	$LiClO_4$ in propylene carbonate	–
C-MO//C	Foo et al., 2014 [228]	0,625	1,22	graphene/V_2O_5	graphene	$LiClO_4$ in propylene carbonate	–
C//C-MO	Bonso et al., 2012 [229]	4	10	activated carbon cloth	graphite nanoplatelet and V_2O_5 nanotubes	LiTFSI in acetonitrile	–

Table 3
Performances of literature-reported devices with ionic liquid electrolytes.

Type	References	Power density, kW/kg	Energy density, Wh/kg	Positive electrode	Negative electrode	Electrolyte	Additional Remarks
C//C	Wang et al., 2018 [78]	61	56	carbon nanomesh constructed by interconnected carbon nanocages derived from sucrose and $Ni(NO_3)_2$	carbon nanomesh constructed by interconnected carbon nanocages derived from sucrose and $Ni(NO_3)_2$	$EMIMBF_4$	more than 90% capacitance retention after 10 000 cycles; PTFE was used as a binder and carbon black as a conductive additive
C//MO	Wang et al., 2017 [230]	20,8	19,1	MnO2 (with 33% wt, of reduced graphene oxide)	activated carbon	$[C_2MIM]BF_4$	PVDF was used as a binder in the negative electrode and acetylene black as a conducting additive
C//CP	Balducci et al., 2005 [231]	1,9	14	poly(3-methylthiophene) (pMeT)	activated carbon	$PYR_{14}TFSI$	90% of capacitance retention after 16 000 cycles
C–C//C–C	Iamprasertkun, 2016 [232]	1,5	245	N-doped reduced graphene oxide aerogel on carboxyl- modified carbon fibre paper		[BMP]-[DCA]	–
C-MO//C-MO	Pendashteh et al., 2017 [233]	7,5	16	electrodes based on MnO_2 nanoparticles grown on macroscopic carbon nanotube fibres		$PYR_{14}TFSI$	90% of capacitance retention after 6 000 cycles
C-CP//C-CP	Wu et al., 2015 [234]	2,4	7,5	alternating stacked graphene-conducting polymer		$EMIMBF_4$	values estimated through the stated density of the electrode material (1.67 g/cm^3)
MO-MO//MO-MO	Chen et al., 2013 [235]	112	20	MnO_2 at nanoporous gold		EMI-DCA	–
MO-CP//MO-CP	Hashmi, 2013 [236]	3,2	0,9	PEDOT-PSS-Ru		PVA- PVP/ $EMIHSO_4$	–
CP-CP//CP-CP	Chen et al., 2013 [237]	158,5	25,1	PAni nanotubes		$EMIMBF_4$	Values extracted from the Ragone plot
MO-C//C	Shen et al., 2016 [238]	12,6	63	polyaniline-derived carbon nanorods	RuO_2 nanodots/reduced graphene oxide (RGO) composite	$EMIM-BF_4$	98.5% capacitance retention after 100 000 cycles
C-CP//C	Cheng et al., 2013 [239]	15,8	14	graphene/CNT	graphene/CNT-PANI	EMI-TFSI	82% of capacitance retention after 1 000 cycles
C-MO//C	Zhang et al., 2013 [240]	10	25	CNT/Au/MnO_2 on nickel foam	activated carbon	$[BMIM]PF_6$/ DMF	–

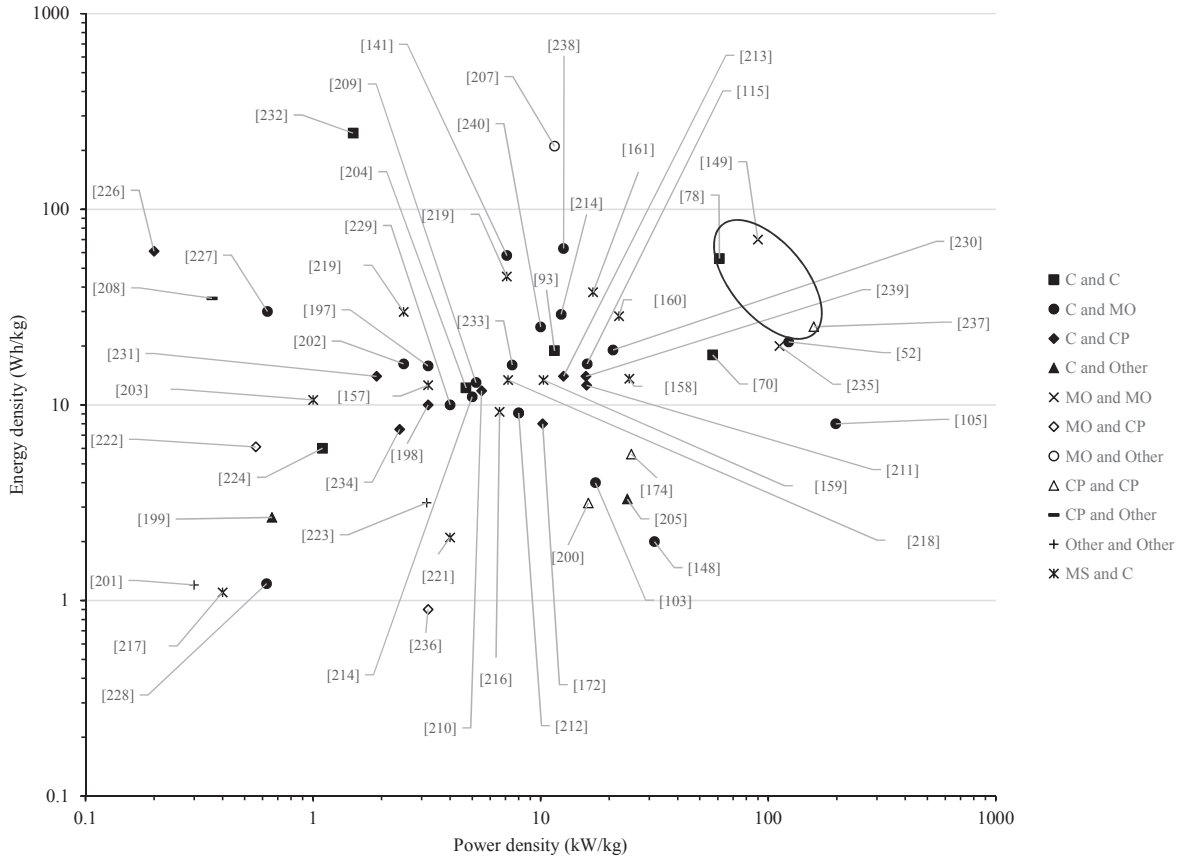

Fig. 3. Ragone plot showing the performances of the devices mentioned in Tables 1a and 1b, 2 and 3, grouped by the type of electrode materials (regardless of being in a symmetric or asymmetric configuration). The values of power and energy densities that did not correspond to the same point ([206;225]) were not included.

- the identification of the current research trends: hybrid supercapacitors with electrodes made of carbon–metal oxide composites and supercapacitors with aqueous electrolytes;
- the identification of some high performing devices: the ones reported by Wang et al. [78], Chen et al. [149] and by Chen et al. [237].

Both Chen et al. [237] and Wang et al. [78] produced symmetric devices with an ionic liquid – $EMIMBF_4$. However, whilst the former reports the fabrication of pseudocapacitors (electrodes made of PAni nanotubes), the latter describes the production of purely capacitive devices (electrodes made of carbon nanomeshes constructed by interconnected carbon nanocages). In both of these studies, the supercapacitors benefitted from tailored electrode structures. Yet, in the report by Wang et al. [78], the device seems to be much more resilient to the increase of the discharge current (maintaining an almost constant energy density) than in the report by Chen et al. [237]. Unsurprisingly, the carbon-based device also presented a much higher cyclability (> 90% of capacitance retention after 10 000 cycles vs ≈45%).

The aqueous electrolyte supercapacitor reported by Chen et al. in [149], despite having a much narrower potential window (1.6 V vs 3.5 V) , achieved an even better performance than the carbon-based device mentioned above. This is probably due to the pronounced faradaic contribution of the electrode materials (RuO_2 and $Co(OH)_2$). As far as cyclability is concerned, it performed worse, only retaining 78% of its capacitance after 3000 cycles.

7. Bottlenecks for the transition from lab to commercial scale

Many literature-reported devices have claimed to achieve remarkably high performances in terms of gravimetric power and energy. In some cases, the obtained energy densities were allegedly comparable to [241] or even higher [211] than the typical energy densities of commercial Li-ion batteries (> 100 Wh/kg [242]). As already discussed, these exciting results should be taken cautiously since there are many differences between a lab-scale supercapacitor and a commercial device (namely the mass that is considered in the calculations and the thickness of the electrode). Yet, even after applying the correction factors needed to extrapolate the device's performance from its active electrode materials, it becomes clear that some of these innovative materials and architectures, if integrated into a device, would actually outperform the commercially available supercapacitors.

Then, how to explain the lasting hegemony of mediocre activated carbon-based supercapacitors in the market? The jump from invention to an innovative product encompasses all the steps required to make an invention into a product. This section intends to briefly analyse some of these and to discuss potential strategies to tackle those limitations.

7.1. Cost of materials (electrodes/electrolytes)

The cost of the materials is inevitably a limiting factor. According to a study reported by Dura et al. [243] in 2013, about 60% − 70% of the production cost of a supercapacitor is related to material costs. And these can be both related to the availability of the raw material and to processing.

Ruthenium oxide is an illustrative example of a high rate active electrode material whose cost (7638 €/kg [244]; activated carbon, for comparison, costs around 13 €/kg [122]) is directly related to its scarcity [245]. Thus, to tackle this problem, cost-effective similar materials have been studied. As already mentioned, manganese oxide is one of the pseudocapacitive materials most often used. However, low conductivity [246] and cycling stability are a significant drawback.

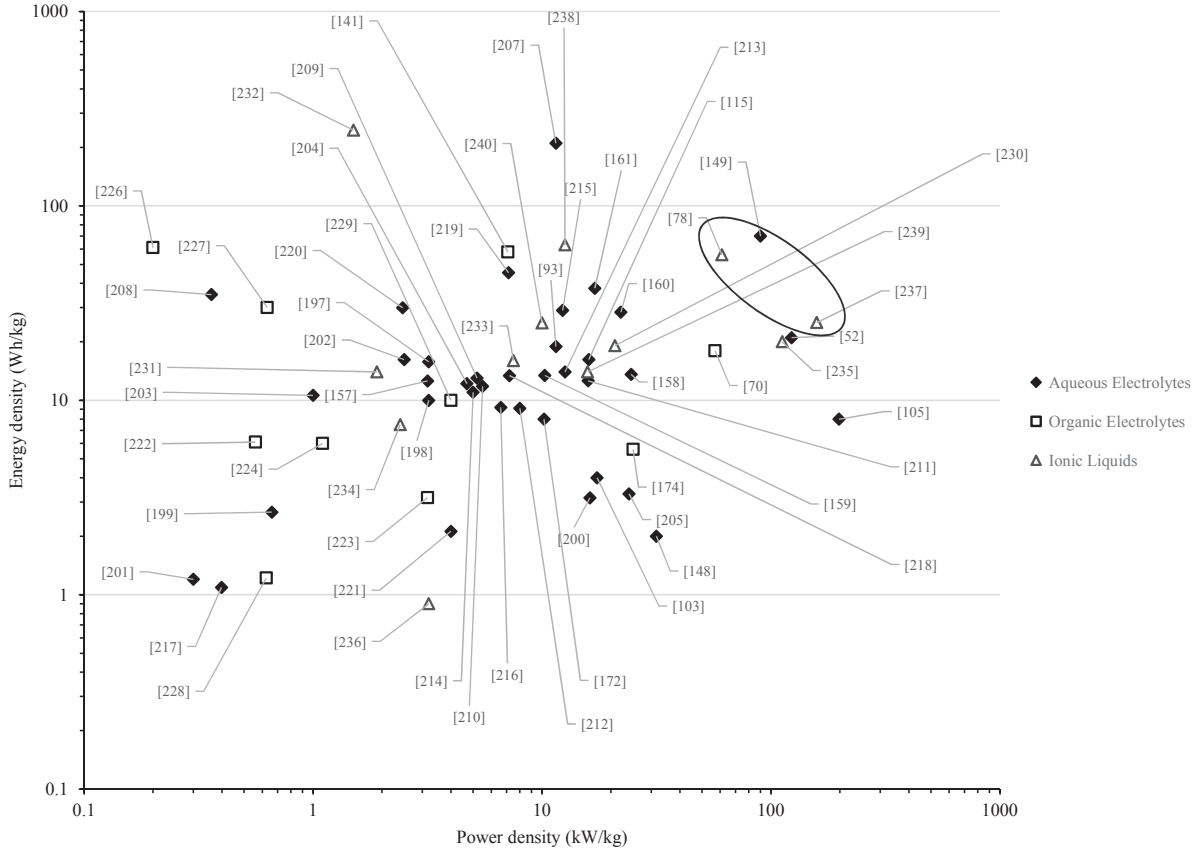

Fig. 4. Ragone plot showing the performances of the devices mentioned in Tables 1a and 1b, Table 2 and Table 3, grouped by the type of electrolyte. The values of power and energy densities that did not correspond to the same point ([206;225]) were not included.

Other promising candidates include niobium oxide [27,247], molybdenum oxide [248], vanadium oxide [249] and nanostructured cobalt ferrite thin films [250]. The recently discovered 2D MXenes (such as $Ti_3C_2T_x$) are also very attractive pseudocapacitive materials, whose capacitance (in aqueous electrolytes) can be as high as 1500F/cm^3 [251]. However, much lower values were obtained for non-aqueous electrolytes (245F/cm^3 in organic electrolytes [193] and 7F/cm^3 [13][252] in ionic liquids) which limits the operative voltage ranges and, consequently, the deliverable energy.

Another less explored idea to potentially reduce the material cost (as well as its environmental impact) is to recycle. Insofar there are no reports concerning Ru based devices. Vermisoglou et al. [253] have shown the technical feasibility of recovering some of the materials used in an EDLC. The authors successfully recovered around 70% of the electrolyte ($TEABF_4$), 59% of the solvent (ACN) and the electrode material (a mixture of activated charcoal and CNT) was also recovered without significant structural changes – the recycled carbonaceous material still exhibited a supercapacitor behaviour. Given the current context of intense resource depletion, the possibility of recycling should always be considered (recycling of lithium-ion batteries is now of high importance [254,255]). Nonetheless, more studies are required to fully assess the economic feasibility of recovering expensive and/or pollutant materials from supercapacitors.

The cost of the raw material is not always the problem. For example, graphene is usually obtained from graphite (relatively inexpensive raw material: 0.73–1.68 €/kg, depending on the flake size [256]). However, processing graphite into graphene is still a cost burden, though it can vary significantly depending on the production method and on its consequent quality [257]. In some applications, lower quality (and inexpensive) graphene can be used. However, energy-related applications typically require near-pristine graphene, often obtained through mechanical exfoliation of graphite, which presents low yields and consequently inflated costs. Nonetheless, this is rapidly changing, with various potentially up-scalable methods to produce high quality graphene being recently reported in the literature: large-scale graphite exfoliation via a simple stirring process in urea/glycerol [258], one-step solvent interface trapping [259], pulsed laser assisted fabrication of graphene nanosheets in water [260], self-propagating high-temperature synthesis of mesoporous graphene from CO_2 [261], nanoclay-assisted electrochemical exfoliation of pencil cores [262], etc.

7.2. Complex manufacturing protocols

Openly accessible information about the industrial production of supercapacitors is scarce. Yet, it is generally known that the main manufacturing steps to obtain a common cylindrical cell are the following [263,264]:

1) Weighing the electrode materials (the active material - often activated carbon; a conducting additive – usually carbon black; and a binder – typically PTFE or PVDF);
2) Mixing the active material with the conductive additive powders (dry mixing) and then, mixing the previously obtained powder mixture with the binder and with an organic solvent – usually NMP or propylene carbonate – to obtain a slurry (wet mixing);
3) Coating the current collectors (often aluminium foil is preferred though stainless steel or nickel -more expensive- are required when corrosive electrolytes are used). This step can be achieved via lithographic or flexographic printing [265];

[13] Value estimated from the density of the material (0.1 g/cm^3), implicit in the article.

4) Drying the coated foil in order to evaporate the solvents used to produce the slurry;
5) Roll pressing the electrode-coated foil to ensure good adhesion of the active material to the current collector foil;
6) Cutting the coated foil with the desired dimensions for the electrodes;
7) Ultrasonically welding the leads to the current collector;
8) Sandwiching a separator paper between two electrodes;
9) Winding the sandwich and soaking it in the electrolyte;
10) Inserting the wet cell in the case, placing a rubber seal on the leads and sealing the cell (steps performed under a controlled atmosphere, and, in the case of organic electrolytes, moisture-free).

When manufacturing coin or pouched cells, the final steps of the process are slightly different (A. Ajina [263] provides further details about these issues), but all of them share a common step for the production of the electrode: formation of a slurry from the powdered active materials and conductive additives. Current industrial production of supercapacitor electrodes is therefore based on a very simple "one-step synthesis". This does not signify that more complex methods to produce electrodes cannot be adopted but adding more steps or significantly modifying the already existing ones inevitably requires additional investment costs in machinery, human resources and/or in raw materials and potentially increases the manufacturing time – both of these resulting in an increased production cost. Increasing the production cost might be worthwhile as long as the performance of the obtained supercapacitor (in terms of cyclability and energy and power densities) also increases accordingly. In this case, the device can be sold for a higher value but still keep its cost per cycle, per Wh and per W[14] – hence preserving profitability and market competitiveness.

Several recently reported supercapacitors with highly optimized electrodes, if transformed into commercial devices, could (even after applying the necessary weight and electrode thickness corrections) result in a 2-fold increase in the energy and/or power density when compared to currently available supercapacitors. However, the syntheses of these optimized electrodes are long, complex and energy intensive. For example, Yao et al. [266] fabricated a supercapacitor where MOF-derived nanoporous carbon (MOF-NPC) was used as negative electrode and MOF-NPC with MnO_2 as the positive electrode (the electrodes were soaked in a neutral aqueous Na_2SO_4 electrolyte). The asymmetric device reached a power density of 22 kW/kg at an energy density of almost 50 Wh/kg. However, in order to obtain these electrodes, the MOF precursor first had to be prepared through a method that, albeit simple, required a 24 h time-step [267]. Subsequently, in order to derive the nanoporous carbon from the MOF powders, a long thermal annealing step, followed by washing, an overnight drying and a high-temperature carbonization was carried out. Du et al. [97] recently produced supercapacitors with an energy density almost as high, 40 Wh/kg (although with a lower corresponding power density, 7 kW/kg). The device was composed of an activated carbon negative electrode and a positive electrode with a 3D heterostructure composed of exfoliated Ni-Al layered double hydroxide nanosheet and reduced graphene oxide (Ni-Al LDH/rGO). The electrodes were soaked in a KOH electrolyte. The rationally designed positive electrode involved a long synthetization process, requiring many time- and energy-consuming steps (e.g. maintaining a solution at 140 °C for 14 h, stirring solutions under N_2 for 3 days, etc.). These examples illustrate that carefully architectured electrodes with optimized performances often come at the expense of long, complex and multiple-step synthetization processes which are impractical for large scale production.

One-step synthesis is highly desirable because of the cost saving potential. A successful example can be found in Yuan et al. [268], where 2D-layered carbon wrapped transition metal nitrides were obtained from transition metal carbides. Although the production of the Ti_3C_2 MXene from Ti_3AlC_2 involves a long HF-etching step, the subsequent route from Ti_3C_2 to the final electrode material via nitridation is straightforward and leads to high yields – but a modest electrochemical performance. A symmetric device soaked in a KOH electrolyte achieved ca. 5 Wh/kg at a power density of 2.2 kW/kg and a 93% capacitance retention after 10 000 cycles. Mohamed et al. [269] reported a higher performance (7 Wh/kg at a power density of 8 kW/kg) for an asymmetric device comprising an activated carbon on nickel foam (NF) positive electrode and a $NiCo_2S_4$ nanoflakes on NF negative electrode. Both electrode syntheses were one-step. These results are far from the best SC literature reported devices. However, because of their relatively high simplicity, the technology readiness level could be considered closer to maturity. Nevertheless, it is worth stressing that accounting in a chemical synthesis step is not always consensual [270] and some process chemists argue that "atom economy" (the minimization of waste products) is a more important up-scalability indicator than step economy [271].

7.3. Lengthy manufacturing steps

A step that is often present in the production of supercapacitors is a thermal treatment, either to increase the porosity and, consequently, the surface area of the electrode (most often in carbon-based materials) or to anneal the metal oxide thin films and nanostructures for pseudocapacitive electrodes [272]. However, this kind of treatment - typically conducted in an oven or in a furnace – is very time- and energy-intensive since it involves keeping the material at high temperatures (300 to 1000 °C, depending on the material and on the intended effect [273,274]) for several hours – usually more than 2 h [272]. Moreover, this process has a very poor energy efficiency, since the heated volume is much larger than the sample that is being treated. Last but not the least, it requires the substrate to be resistant to high temperatures (this is very restrictive for flexible supercapacitors, whose substrates are usually polymer-based) [275].

All of these disadvantages led to several attempts to find alternatives to the conventional thermal method (intense pulsed light [276], halogen lamp [277], infra-red radiation [278], etc.), but most of them require more than one treatment to yield a complete annealing [279]. On the contrary, laser annealing, by inducing a highly localized heating, seems to achieve even better results in terms of mechanical and electrical properties than conventional thermal annealing, while enabling a significant reduction in the processing time and energy consumption. Yeo et al. [275] demonstrated the feasibility of this technique for the mass production of flexible supercapacitor current collectors, by laser processing a roll-to-roll printed silver nanoparticle ink on a polymer substrate. For comparison, the authors fabricated two almost identical electrodes: a carbon coated laser annealed current collector and a carbon coated thermal annealed current collector made of the same silver nanoparticle ink. The electrochemical behaviour of each one of the electrodes was investigated in a 3-electrode cell configuration where a 1 M Na_2SO_4 solution was used as the electrolyte. The laser annealed electrode showed an overall better performance.

Lasers have also been used to process the active electrode material. For example, P. Simon's team recently fabricated RuO_2 micro-supercapacitor electrodes by laser-scribing a ruthenium organometallic precursor on a flexible substrate [280]. The as-prepared RuO_2 film presented good adherence to the gold-based thin film deposited on the flexible substrate and thus no binding additives were necessary. The obtained electrodes were characterized in a 3-electrode cell configuration and demonstrated a good areal capacitance (16 mF/cm^2 at

[14] It might be difficult to simultaneously increase these three performance indicators and thus the price per one or two of these features might actually increase in a product. Yet, the product might still be competitive in niche markets (e.g. if a certain device provides more expensive power but cheaper cycles, it will be attractive for applications where the cycle life is more important than the power rating).

100 mV/s in 1 M H_2SO_4). Lasers were also successfully used in carbon-based electrode materials. Hwang et al. [93] recently laser-treated activated carbon electrodes and, as a result, obtained an increased capacitance and a reduced internal resistance due to the formation of microchannels that connected the internal pores of the activated carbon with the surrounding electrolyte. The symmetric supercapacitor fabricated with the laser-scribed activated carbon electrodes delivered 18.9 Wh/kg at a power density of 11.5 kW/kg. Yet, it is worth mentioning that this high performance was not exclusively due to the laser treatment; instead, it was the result of a synergistic effect between the laser-processed electrodes and a redox-active electrolyte (containing the [Fe(CN)/Fe(CN)] couple), which enabled a pseudocapacitive contribution and the extension of the operative voltage window.

Yet, the currently most common application of lasers in supercapacitors has been, by far, in the reduction of graphene oxide. Since El-Kady and Kaner reported a simple and scalable technique to fabricate high-power graphene micro-supercapacitors [281], many other similar studies started to appear. These authors successfully obtained more than 100 flexible laser-scribed graphene micro-supercapacitors in 30 min, by etching (with a simple LightScribe DVD burner) the computer-designed interdigitated supercapacitors on a graphene oxide film supported on a PET sheet and placed on a DVD media disc. The areas irradiated by the laser were converted into reduced graphene oxide (i.e. graphene – which, being highly conductive, served simultaneously as active electrode material and as current collector) whilst the rest remained under the form of graphene oxide – which has a much lower conductivity [282]. To complete the micro-supercapacitors, the ionogel electrolyte (an ionic liquid mixed with fumed silica nanopowder) was then drop-cast on the active interdigitated electrode areas. The as-fabricated devices presented a remarkably high power density of 200 W/cm^3. Other authors have used a similar approach to obtain graphene-based supercapacitors. Lin et al. [283] obtained laser-induced porous graphene films from commercial polymers, which were patterned to interdigitated electrodes and used in micro-supercapacitors. The as-fabricated devices presented an areal performance comparable to other similar devices (a capacitance higher than 4 mF/cm^2 and a power density of 9 mW/cm^2). More recently, Liu et al. [284] obtained few-layer graphene polyhedral networks by laser-scribing polyimide sheets. However, instead of using a CO_2-laser (as Lin et al. [283]), the authors used a Nd: YAG semiconductor laser (with a fixed wavelength of 1064 nm). The laser-scribed electrodes were then soaked in a PVA/LiCl gel electrolyte and sandwiched into a symmetric supercapacitor, which demonstrated a high areal capacitance of 34.7 mF/cm^2.

Laser-induced graphene is obtainable via a roll-2-roll process and also by 3-D printing, which are both highly up-scalable techniques [285].

8. Conclusion

Supercapacitors, having the ability to store and provide energy at very high rates and to endure many charge–discharge cycles, will certainly play an important role in future energy storage systems. However, to increase the penetration of these devices in the market of energy storage technologies, the following improvements are still necessary:

1) Their cost of production should be brought down through the optimization of the fabrication methods, including materials synthesis (a key goal is to move towards a fast and efficient “one-step synthesis”) and processing (e.g. obtaining graphene from graphite). A successful reduction of the processing cost will be paramount for the incorporation of new electrode materials (such as graphene) in commercial supercapacitors. Many potentially up-scalable methods to produce high quality graphene have been recently reported in the literature, which increases the likelihood of commercialization. As such, commercially proliferation of supercapactiors incorporating graphene can be expected (e.g. Skeleton© has been having a substantial success with their patented curved graphene technology).
2) The energy density of active materials should be increased through appropriate selection of electrolytes with an extended voltage window (and eventually with redox characteristics) and also through the hybridization between capacitive and pseudocapacitive electrode materials
3) Their structure should become as versatile as possible to enable their integration in a larger number of applications – for this flexible, all-solid-state, and either micro or fibre-shaped supercapacitors appear to be particularly promising.

Also important is a more accurate benchmarking of results – and a consequently clearer identification of the most promising materials and device architectures -, supercapacitor-related articles should adopt more standardized performance characterization.

In particular, it would be advisable to present the results for measurements performed both in a 3- and in a 2- electrode configurations (using the same electrolyte for both setups). Moreover, pre-defined mass loading (10 mg/cm^2 for instance, which is the typical value for commercial devices) should be sought after, since this often-underrated feature largely influences the performance output. Another relevant issue is the number of cycles in the cyclability test and the current density at which this test is performed. Since these devices are expected to endure nearly one million charge–discharge cycles without degradation, the “endurance test” should include a pre-defined and very high number of cycles and the cycles should be undertaken at the highest current density that the device can provide. It is frequent to find in the reported literature that energy and power densities are also determined using different methods which may not yield easily comparable results.

In summary, determining the adequate methods and parameters for a standardized performance assessment is not a trivial task but the authors of this review consider it valuable. An approach would be to take the already existing norms prepared by the International Electrotechnical Commission (IEC) -namely IEC 62576:2018 and IEC 62391-2:2006 – and adapt them to a lab-level context. This way, there would certainly be fewer “outstanding” devices reported in the literature, but it would be simpler to identify the promising ones, which could accelerate the progress in this field. With more reliable performance reporting, it is conceivable that industry would take greater consideration of potential new avenues.

Declaration of Competing Interest

None.

Acknowledgements

This work was supported by Fundação para a Ciência e a Tecnologia, “FCT” (grant PD/BD/128169/2016 and project UID/GEO/50019/2019 - Instituto Dom Luiz) and by the UK EPSRC Joint University Industry Consortium for Energy (Materials) and Devices Hub (EP/R023662/1).

Finally, the authors would like to thank Paulo Luís, Energy Research Laboratory, Department of Chemistry, Loughborough University, UK for all the fruitful discussions.

References

[1] J. Delgado, R. Faria, P. Moura, A.T. de Almeida, Impacts of plug-in electric vehicles in the portuguese electrical grid, Transp. Res. Part D Transp. Environ. 62 (2018) 372–385, https://doi.org/10.1016/J.TRD.2018.03.005.
[2] G. Castagneto Gissey, P.E. Dodds, J. Radcliffe, Market and regulatory barriers to electrical energy storage innovation, Renew. Sustain. Energy Rev. 82 (2018) 781–790, https://doi.org/10.1016/j.rser.2017.09.079.
[3] P. Nikolaidis, A. Poullikkas, Cost metrics of electrical energy storage technologies

in potential power system operations, Sustain. Energy Technol. Assessments. 25 (2018) 43–59, https://doi.org/10.1016/j.seta.2017.12.001.
[4] L. Kouchachvili, W. Yaïci, E. Entchev, Hybrid battery/supercapacitor energy storage system for the electric vehicles, J. Power Sources 374 (2018) 237–248, https://doi.org/10.1016/j.jpowsour.2017.11.040.
[5] N.S. Jayalakshmi, D.N. Gaonkar, P.B. Nempu, Power control of PV/fuel cell/supercapacitor hybrid system for stand-alone applications, Int. J. Renew. ENERGY Res. 6 (2016).
[6] T. Aytug, M.S. Rager, W. Higgins, F.G. Brown, G.M. Veith, C.M. Rouleau, H. Wang, Z.D. Hood, S.M. Mahurin, R.T. Mayes, P.C. Joshi, T. Kuruganti, Vacuum-assisted low-temperature synthesis of reduced graphene oxide thin-film electrodes for high-performance transparent and flexible all-solid-state supercapacitors, ACS Appl. Mater. Interfaces 10 (2018) 11008–11017, https://doi.org/10.1021/acsami.8b01938.
[7] A. Sellam, R.N. Jenjeti, S. Sampath, Ultrahigh-Rate Supercapacitors Based on 2-Dimensional, 1T MoS 2x Se 2(1 − x) for AC Line-Filtering Applications, (n.d.). doi: 10.1021/acs.jpcc.8b01593.
[8] M.E. Suss, S. Porada, X. Sun, P.M. Biesheuvel, J. Yoon, V. Presser, Water desalination via capacitive deionization: what is it and what can we expect from it? Energy Environ. Sci. 8 (2015) 2296–2319, https://doi.org/10.1039/C5EE00519A.
[9] J.R. Miller, A.F. Burke, Electrochemical capacitors: challenges and opportunities for real-world applications, Electrochem. Soc. 17 (2008) 53–57, https://doi.org/10.1201/9781420069709.
[10] L.L. Zhang, X.S. Zhao, Carbon-based materials as supercapacitor electrodes, Chem. Soc. Rev. 38 (2009) 2520, https://doi.org/10.1039/b813846j.
[11] M. Yassine, D. Fabris, Performance of commercially available supercapacitors, Energies 10 (2017), https://doi.org/10.3390/en10091340.
[12] J.R. McGhee, R.B. Middlemiss, D.J. Southee, K.G.U. Wijayantha, P.S.A. Evans, Flexible, All Metal-Oxide Capacitors for Printed Electronics, 2018 IEEE 13th Nanotechnol. Mater. Devices Conf. 2 (2018) 1–4. doi: 10.1109/NMDC.2018.8605872.
[13] T.R. Kuphaldt, Lessons In Electric Circuits Volume I – DC, 2006.
[14] K. Murata, K. Mitsuoka, T. Hirai, T. Walz, P. Agre, J.B. Heymann, a. Engel, Y. Fujiyoshi, Structural determinants of water permeation through aquaporin-1, Nature 407 (6804) (2000) 599–605, https://doi.org/10.1038/35036519.
[15] A. González, E. Goikolea, J.A. Barrena, R. Mysyk, Review on supercapacitors: technologies and materials, Renew. Sustain. Energy Rev. 58 (2016) 1189–1206, https://doi.org/10.1016/j.rser.2015.12.249.
[16] Y.M. Shulga, S.A. Baskakov, V.A. Smirnov, N.Y. Shulga, K.G. Belay, G.L. Gutsev, Graphene oxide films as separators of polyaniline-based supercapacitors, J. Power Sources 245 (2014) 33–36, https://doi.org/10.1016/j.jpowsour.2013.06.094 Short communication.
[17] L. Zubieta, R. Bonert, Characterization of double-layer capacitors for power electronics applications, IEEE Trans. Ind. Appl. 36 (2000) 199–205, https://doi.org/10.1109/28.821816.
[18] L. Zhang, X. Hu, Z. Wang, F. Sun, D.G. Dorrell, A review of supercapacitor modeling, estimation, and applications: a control/management perspective, Renew. Sustain. Energy Rev. 81 (2018) 1868–1878, https://doi.org/10.1016/j.rser.2017.05.283.
[19] F. Rafik, H. Gualous, R. Gallay, A. Crausaz, A. Berthon, Frequency, thermal and voltage supercapacitor characterization and modeling, J. Power Sources 165 (2007) 928–934, https://doi.org/10.1016/j.jpowsour.2006.12.021.
[20] B.E. Conway, Electrochemical Supercapacitors – Scientific Fundamentals and Technological Applications, Springer Science + Business Media, LLC, Ottawa, 1999. doi: 10.1002/9783527639496.ch8.
[21] C.H. Lai, D. Ashby, M. Moz, Y. Gogotsi, L. Pilon, B. Dunn, Designing pseudocapacitance for Nb2O5/carbide-derived carbon electrodes and hybrid devices, Langmuir 33 (2017) 9407–9415, https://doi.org/10.1021/acs.langmuir.7b01110.
[22] Y. Shi, L. Peng, Y. Ding, Y. Zhao, G. Yu, Nanostructured conductive polymers for advanced energy storage, Chem. Soc. Rev. 44 (2015) 6684–6696, https://doi.org/10.1039/c5cs00362h.
[23] G.Z. Chen, Supercapacitor and supercapattery as emerging electrochemical energy stores, Int. Mater. Rev. 62 (2017) 173–202, https://doi.org/10.1080/09506608.2016.1240914.
[24] G. Yu, X. Xie, L. Pan, Z. Bao, Y. Cui, Hybrid nanostructured materials for high-performance electrochemical capacitors, Nano Energy 2 (2013) 213–234, https://doi.org/10.1016/j.nanoen.2012.10.006.
[25] T. Brousse, B. Daniel, To be or not to be pseudocapacitive? J. Electrochem. Soc. 162 (2015) 5185–5189, https://doi.org/10.1149/2.0201505jes.
[26] H. Li, L. Peng, Y. Zhu, X. Zhang, G. Yu, Achieving high-energy-high-power density in a flexible quasi-solid-state sodium ion capacitor, Nano Lett. 16 (2016) 5938–5943, https://doi.org/10.1021/acs.nanolett.6b02932.
[27] H. Li, Y. Zhu, S. Dong, L. Shen, Z. Chen, X. Zhang, G. Yu, Self-Assembled Nb2O5 nanosheets for high energy-high power sodium ion capacitors, Chem. Mater. 28 (2016) 5753–5760, https://doi.org/10.1021/acs.chemmater.6b01988.
[28] K. Chen, D. Xue, How to efficiently utilize electrode materials in supercapattery? Funct. Mater. Lett. 12 (2018) 1830005, https://doi.org/10.1142/s1793604718300050.
[29] K. Chen, D. Xue, Colloidal paradigm in supercapattery electrode systems, Nanotechnology 29 (2018), https://doi.org/10.1088/1361-6528/aa9bfd.
[30] X. Chen, K. Chen, H. Wang, D. Xue, A colloidal pseudocapacitor: Direct use of Fe (NO3)3 in electrode can lead to a high performance alkaline supercapacitor system, J. Colloid Interface Sci. 444 (2015) 49–57, https://doi.org/10.1016/j.jcis.2014.12.026.
[31] K. Chen, F. Liu, X. Liang, D. Xue, Surface-interface reaction of supercapacitor electrode materials, Surf. Rev. Lett. 24 (2017) 1730005, https://doi.org/10.1142/s0218625x17300052.
[32] K. Chen, D. Xue, Colloidal supercapacitor electrode materials, Mater. Res. Bull. 83 (2016) 201–206, https://doi.org/10.1016/j.materresbull.2016.06.013.
[33] K. Chen, G. Li, D. Xue, Architecture engineering of supercapacitor electrode materials, Funct. Mater. Lett. 09 (2016) 1640001, https://doi.org/10.1142/s1793604716400014.
[34] K. Chen, D. Xue, Materials chemistry toward electrochemical energy storage, J. Mater. Chem. A. 4 (2016) 7522–7537, https://doi.org/10.1039/c6ta01527a.
[35] K.F. Chen, D.F. Xue, Rare earth and transitional metal colloidal supercapacitors, Sci. China Technol. Sci. 58 (2015) 1768–1778, https://doi.org/10.1007/s11431-015-5915-z.
[36] V.V.N. Obreja, Supercapacitors specialities – materials review, AIP Conf. Proc. 1597 (2014) 98–120, https://doi.org/10.1063/1.4878482.
[37] IEC (International Electrotechnical Commission), International Standard: Fixed electric double-layer capacitors for use in electronic equipment, 2006.
[38] M.D. Stoller, R.S. Ruoff, Best practice methods for determining an electrode material's performance for ultracapacitors, Energy Environ. Sci. 3 (2010) 1294, https://doi.org/10.1039/c0ee00074d.
[39] D.W. Wang, F. Li, M. Liu, G.Q. Lu, H.M. Cheng, 3D aperiodic hierarchical porous graphitic carbon material for high-rate electrochemical capacitive energy storage, Angew. Chemie – Int. Ed. 47 (2008) 373–376, https://doi.org/10.1002/anie.200702721.
[40] J. Chmiola, Anomalous increase in carbon capacitance at pore sizes less than 1 nanometer, Science 313 (5794) (2006) 1760–1763.
[41] J. Dzubiella, J.P. Hansen, Electric-field-controlled water and ion permeation of a hydrophobic nanopore, J. Chem. Phys. 122 (2005), https://doi.org/10.1063/1.1927514.
[42] J. Huang, B.G. Sumpter, V. Meunier, A universal model for nanoporous carbon supercapacitors applicable to diverse pore regimes, carbon materials, and electrolytes, Chem. – A Eur. J. 14 (2008) 6614–6626, https://doi.org/10.1002/chem.200800639.
[43] M. Seredych, D. Hulicova-Jurcakova, G.Q. Lu, T.J. Bandosz, Surface functional groups of carbons and the effects of their chemical character, density and accessibility to ions on electrochemical performance, Carbon N. Y. 46 (2008) 1475–1488, https://doi.org/10.1016/j.carbon.2008.06.027.
[44] F. Béguin, V. Presser, A. Balducci, E. Frackowiak, Carbons and electrolytes for advanced supercapacitors, Adv. Mater. 26 (2014) 2219–2251, https://doi.org/10.1002/adma.201304137.
[45] C. Hung, C. Yang, J. Lin, S. Huang, Y. Chang, S. Liu, New Insights Into the Operating Voltage of Aqueous Supercapacitors, 2016. doi:10.1016/j.micromeso.2016.03.006.This.
[46] R. Kötz, M. Carlen, Principles and applications of electrochemical capacitors, Electrochim. Acta. 45 (2000) 2483–2498, https://doi.org/10.1016/S0013-4686(00)00354-6.
[47] Y.J. Kim, Y. Horie, S. Ozaki, Y. Matsuzawa, H. Suezaki, C. Kim, N. Miyashita, M. Endo, Correlation between the pore and solvated ion size on capacitance uptake of PVDC-based carbons, Carbon N. Y. 42 (2004) 1491–1500, https://doi.org/10.1016/j.carbon.2004.01.049.
[48] M.P. Bichat, E. Raymundo-Piñero, F. Béguin, High voltage supercapacitor built with seaweed carbons in neutral aqueous electrolyte, Carbon N. Y. 48 (2010) 4351–4361, https://doi.org/10.1016/j.carbon.2010.07.049.
[49] C. Wessells, R. Ruffo, R.A. Huggins, Y. Cui, Investigations of the electrochemical stability of aqueous electrolytes for lithium battery applications, Electrochem. Solid-State Lett. 13 (2010) A59, https://doi.org/10.1149/1.3329652.
[50] H. Tomiyasu, H. Shikata, K. Takao, N. Asanuma, S. Taruta, Y.-Y. Park, An aqueous electrolyte of the widest potential window and its superior capability for capacitors, Sci. Rep. 7 (2017) 45048, https://doi.org/10.1038/srep45048.
[51] J. Cao, Y. Wang, Y. Zhou, J.H. Ouyang, D. Jia, L. Guo, High voltage asymmetric supercapacitor based on MnO2 and graphene electrodes, J. Electroanal. Chem. 689 (2013) 201–206, https://doi.org/10.1016/j.jelechem.2012.10.024.
[52] V. Khomenko, E. Raymundo-Piñero, F. Béguin, Optimisation of an asymmetric manganese oxide/activated carbon capacitor working at 2 v in aqueous medium, J. Power Sources. 153 (2006) 183–190, https://doi.org/10.1016/j.jpowsour.2005.03.210.
[53] C. Du, J. Yeh, N. Pan, High power density supercapacitors using locally aligned carbon nanotube electrodes, Nanotechnology 16 (2005) 350–353, https://doi.org/10.1088/0957-4484/16/4/003.
[54] M. Kaempgen, C.K. Chan, J. Ma, Y. Cui, G. Gruner, Printable Thin Film Supercapacitors Using Single-Walled Carbon Nanotubes 2009, 2009. doi: 10.1021/nl8038579.
[55] A. Izadi-najafabadi, T. Yamada, D.N. Futaba, M. Yudasaka, H. Takagi, H. Hatori, High-power supercapacitor electrodes nanotube from single-walled carbon nanohorn/nanotube composite, ACS Nano 5 (2011) 811–819, https://doi.org/10.1021/nn1017457.
[56] D.P. Dubal, O. Ayyad, V. Ruiz, P. Gómez-Romero, Hybrid energy storage: the merging of battery and supercapacitor chemistries, Chem. Soc. Rev. 44 (2015) 1777–1790, https://doi.org/10.1039/C4CS00266K.
[57] J.S. Sagu, K.G.U. Wijayantha, M. Bohm, S. Bohm, T. Kumar Rout, Anodized steel electrodes for supercapacitors, ACS Appl. Mater. Interfaces. 8 (2016) 6277–6285, https://doi.org/10.1021/acsami.5b12107.
[58] K.M. Hercule, Q. Wei, A.M. Khan, Y. Zhao, X. Tian, L. Mai, Synergistic effect of hierarchical nanostructured MoO2/Co(OH)2 with largely enhanced pseudocapacitor cyclability, Nano Lett. 13 (2013) 5685–5691, https://doi.org/10.1021/nl403372n.
[59] N. Dukstiene, D. Sinkeviciute, A. Guobiene, Morphological, structural and optical properties of MoO2 films electrodeposited on SnO2|glass plate, Open Chem. 10

(2012), https://doi.org/10.2478/s11532-012-0012-7.
[60] Z. Wu, X.L. Huang, Z.L. Wang, J.J. Xu, H.G. Wang, X.B. Zhang, Electrostatic induced stretch growth of homogeneous β-Ni(OH) 2 on graphene with enhanced high-rate cycling for supercapacitors, Sci. Rep. 4 (2014) 1–8, https://doi.org/10.1038/srep03669.
[61] Y. Gao, Graphene and polymer composites for supercapacitor applications: a review, Nanoscale Res. Lett. 12 (2017) 387, https://doi.org/10.1186/s11671-017-2150-5.
[62] Y. Shi, X. Zhou, G. Yu, Material and structural design of novel binder systems for high-energy, high-power lithium-ion batteries, Acc. Chem. Res. 50 (2017) 2642–2652, https://doi.org/10.1021/acs.accounts.7b00402.
[63] C. Zhong, Y. Deng, W. Hu, J. Qiao, L. Zhang, J. Zhang, A review of electrolyte materials and compositions for electrochemical supercapacitors, Chem. Soc. Rev. 44 (2015) 7484–7539, https://doi.org/10.1039/C5CS00303B.
[64] X. Zang, C. Shen, M. Sanghadasa, L. Lin, High-voltage supercapacitors based on aqueous electrolytes, ChemElectroChem. (2018), https://doi.org/10.1002/celc.201801225.
[65] T. Xiong, T.L. Tan, L. Lu, W.S.V. Lee, J. Xue, Harmonizing energy and power density toward 2.7 V asymmetric aqueous supercapacitor, Adv. Energy Mater. 1702630 (2018) 1–10, https://doi.org/10.1002/aenm.201702630.
[66] J.Y. Hwang, M.F. El-Kady, M. Li, C.W. Lin, M. Kowal, X. Han, R.B. Kaner, Boosting the capacitance and voltage of aqueous supercapacitors via redox charge contribution from both electrode and electrolyte, Nano Today 15 (2017) 15–25, https://doi.org/10.1016/j.nantod.2017.06.009.
[67] Y.Z. Wu, Y. Ding, T. Hayat, A. Alsaedi, S.Y. Dai, Enlarged working potential window for MnO2 supercapacitors with neutral aqueous electrolytes, Appl. Surf. Sci. 459 (2018) 430–437, https://doi.org/10.1016/j.apsusc.2018.07.147.
[68] M. Galiński, A. Lewandowski, I. Stepniak, Ionic liquids as electrolytes, Electrochim. Acta. 51 (2006) 5567–5580, https://doi.org/10.1016/j.electacta.2006.03.016.
[69] M.F. Hsueh, C.W. Huang, C.A. Wu, P.L. Kuo, H. Teng, The synergistic effect of nitrile and ether functionalities for gel electrolytes used in supercapacitors, J. Phys. Chem. C. 117 (2013) 16751–16758, https://doi.org/10.1021/jp4031128.
[70] S. Ahmed, A. Ahmed, M. Rafat, Impact of aqueous and organic electrolytes on the supercapacitive performance of activated carbon derived from pea skin, Surf. Coatings Technol. 349 (2018) 242–250, https://doi.org/10.1016/j.surfcoat.2018.05.073.
[71] A. Brandt, S. Pohlmann, A. Varzi, A. Balducci, S. Passerini, Ionic liquids in supercapacitors, MRS Bull. 38 (2013) 554–559, https://doi.org/10.1557/mrs.2013.151.
[72] R.D. Rogers, G.A. Voth, Ionic liquids, Acc. Chem. Res. 40 (2007) 1077–1078, https://doi.org/10.1049/iet-rpg.2016.0914.
[73] M. Armand, F. Endres, D.R. MacFarlane, H. Ohno, B. Scrosati, Ionic-liquid materials for the electrochemical challenges of the future, Nat. Mater. 8 (2009) 621–629, https://doi.org/10.1038/nmat2448.
[74] S. Fletcher, V.J. Black, I. Kirkpatrick, T.S. Varley, Quantum design of ionic liquids for extreme chemical inertness and a new theory of the glass transition, J. Solid State Electrochem. 17 (2013) 327–337, https://doi.org/10.1007/s10008-012-1974-2.
[75] K.L. Van Aken, M. Beidaghi, Y. Gogotsi, Formulation of ionic-liquid electrolyte to expand the voltage window of supercapacitors, Angew. Chemie – Int. Ed. 54 (2015) 4806–4809, https://doi.org/10.1002/anie.201412257.
[76] A.M.O. Mahony, D.S. Silvester, L. Aldous, C. Hardacre, R.G. Compton, Effect of water on the electrochemical window and potential limits of room-temperature ionic liquids effect of water on the electrochemical window and potential limits of room-temperature ionic liquids, Engineering 2884–2891 (2008).
[77] R. Thangavel, A.G. Kannan, R. Ponraj, V. Thangavel, D.W. Kim, Y.S. Lee, High-energy green supercapacitor driven by ionic liquid electrolytes as an ultra-high stable next-generation energy storage device, J. Power Sources 383 (2018) 102–109, https://doi.org/10.1016/j.jpowsour.2018.02.037.
[78] D. Wang, Y. Wang, H. Liu, W. Xu, L. Xu, Unusual carbon nanomesh constructed by interconnected carbon nanocages for ionic liquid-based supercapacitor with superior rate capability, Chem. Eng. J. 342 (2018) 474–483, https://doi.org/10.1016/j.cej.2018.02.085.
[79] B.E. Francisco, C.M. Jones, S.-H. Lee, C.R. Stoldt, Nanostructured all-solid-state supercapacitor based on Li $_2$ S-P $_2$ $_S$ 5 glass-ceramic electrolyte, Appl. Phys. Lett. 100 (2012) 103902, https://doi.org/10.1063/1.3693521.
[80] A.S. Ulihin, N.F. Uvarov, Y.G. Mateyshina, L.I. Brezhneva, A.A. Matvienko, Composite solid electrolytes LiClO4-Al2O3, Solid State Ionics 177 (2006) 2787–2790, https://doi.org/10.1016/j.ssi.2006.03.018.
[81] S. Roldán, M. Granda, R. Menéndez, R. Santamaría, C. Blanco, Mechanisms of energy storage in carbon-based supercapacitors modified with a quinoid redox-active electrolyte, J. Phys. Chem. C. 115 (2011) 17606–17611, https://doi.org/10.1021/jp205100v.
[82] S. Roldán, Z. González, C. Blanco, M. Granda, R. Menéndez, R. Santamaría, Redox-active electrolyte for carbon nanotube-based electric double layer capacitors, Electrochim. Acta. 56 (2011) 3401–3405, https://doi.org/10.1016/j.electacta.2010.10.017.
[83] L. Chen, Y. Chen, J. Wu, J. Wang, H. Bai, L. Li, Electrochemical supercapacitor with polymeric active electrolyte, J. Mater. Chem. A. 2 (2014) 10526–10531, https://doi.org/10.1039/C4TA01319K.
[84] S. Roldán, M. Granda, R. Menéndez, R. Santamaría, C. Blanco, Supercapacitor modified with methylene blue as redox active electrolyte, Electrochim. Acta 83 (2012) 241–246, https://doi.org/10.1016/j.electacta.2012.08.026.
[85] K. Chen, D. Xue, Colloidal supercapattery: redox ions in electrode and electrolyte, Chem. Rec. 18 (2018) 282–292, https://doi.org/10.1002/tcr.201700037.
[86] L. Chen, H. Bai, Z. Huang, L. Li, Mechanism investigation and suppression of self-discharge in active electrolyte enhanced supercapacitors, Energy Environ. Sci. 7 (2014) 1750–1759, https://doi.org/10.1039/C4EE00002A.
[87] N. Dubouis, P. Lemaire, B. Mirvaux, E. Salager, M. Deschamps, A. Grimaud, The role of the hydrogen evolution reaction in the solid–electrolyte interphase formation mechanism for " *Water-in-Salt* " electrolytes, Energy Environ. Sci. (2018) 3491–3499, https://doi.org/10.1039/C8EE02456A.
[88] L. Suo, O. Borodin, T. Gao, M. Olguin, J. Ho, X. Fan, C. Luo, C. Wang, K. Xu, "Water-in-salt" electrolyte enables high-voltage aqueous lithium-ion chemistries, Science 350 (6263) (2015) 938–943, https://doi.org/10.1126/science:aab1595.
[89] M. Watanabe, M.L. Thomas, S. Zhang, K. Ueno, T. Yasuda, K. Dokko, Application of ionic liquids to energy storage and conversion materials and devices, Chem. Rev. 117 (2017) 7190–7239, https://doi.org/10.1021/acs.chemrev.6b00504.
[90] P. Lannelongue, R. Bouchal, E. Mourad, C. Bodin, M. Olarte, S. le Vot, F. Favier, O. Fontaine, "Water-in-Salt" for supercapacitors: a compromise between voltage, power density, energy density and stability, J. Electrochem. Soc. 165 (2018) A657–A663, https://doi.org/10.1149/2.0951803jes.
[91] K. Jurewicz, C. Vix-Guterl, E. Frackowiak, S. Saadallah, M. Reda, J. Parmentier, J. Patarin, F. Béguin, Capacitance properties of ordered porous carbon materials prepared by a templating procedure, J. Phys. Chem. Solids. 65 (2004) 287–293, https://doi.org/10.1016/j.jpcs.2003.10.024.
[92] P. Simon, A. Burke, Nanostructured carbons: double-layer capacitance and more, Electrochem. Soc. Interface. 17 (2008) 38–43, https://doi.org/10.1016/j.carbon.2005.06.046.
[93] J.Y. Hwang, M. Li, M.F. El-Kady, R.B. Kaner, Next-generation activated carbon supercapacitors: a simple step in electrode processing leads to remarkable gains in energy density, Adv. Funct. Mater. 27 (2017), https://doi.org/10.1002/adfm.201605745.
[94] C.J. Raj, M. Rajesh, R. Manikandan, K.H. Yu, J.R. Anusha, J.H. Ahn, D.W. Kim, S.Y. Park, B.C. Kim, High electrochemical capacitor performance of oxygen and nitrogen enriched activated carbon derived from the pyrolysis and activation of squid gladius chitin, J. Power Sources. 386 (2018) 66–76, https://doi.org/10.1016/j.jpowsour.2018.03.038.
[95] Z. Wu, X. Zhang, N, O-codoped porous carbon nanosheets for capacitors with ultra-high capacitance氮氧共掺杂多孔碳片用于超高比容量的超级电容器, Sci. China Mater. 59 (2016) 547–557, https://doi.org/10.1007/s40843-016-5067-4.
[96] H. Kim, M.Y. Cho, M.H. Kim, K.Y. Park, H. Gwon, Y. Lee, K.C. Roh, K. Kang, A novel high-energy hybrid supercapacitor with an anatase tio 2-reduced graphene oxide anode and an activated carbon cathode, Adv. Energy Mater. 3 (2013) 1500–1506, https://doi.org/10.1002/aenm.201300467.
[97] Q. Du, L. Su, L. Hou, G. Sun, M. Feng, X. Yin, Z. Ma, G. Shao, W. Gao, Rationally designed ultrathin Ni-Al layered double hydroxide and graphene heterostructure for high-performance asymmetric supercapacitor, J. Alloys Compd. 740 (2018) 1051–1059, https://doi.org/10.1016/j.jallcom.2018.01.069.
[98] Y. Gogotsi, P. Simon, True performance metrics in electrochemical energy storage, Science 334 (6058) (2011) 917–918, https://doi.org/10.1126/science:1213003.
[99] H. Tavanai, R. Jalili, M. Morshed, Effects of fiber diameter and CO2 activation temperature on the pore characteristics of polyacrylonitrile based activated carbon nanofibers, Surf. Interface Anal. 41 (2009) 814–819, https://doi.org/10.1002/sia.3104.
[100] G. Moreno-fernandez, J. Ibañez, J.M. Rojo, M. Kunowsky, Activated Carbon Fiber Monoliths as Supercapacitor Electrodes, 2017 (2017). doi: 10.1155/2017/3625414.
[101] B. Xu, F. Wu, R. Chen, G. Cao, S. Chen, Z. Zhou, Y. Yang, Highly mesoporous and high surface area carbon: a high capacitance electrode material for EDLCs with various electrolytes, Electrochem. Commun. 10 (2008) 795–797, https://doi.org/10.1016/j.elecom.2008.02.033.
[102] N. Yu, H. Yin, W. Zhang, Y. Liu, Z. Tang, M.Q. Zhu, High-performance fiber-shaped all-solid-state asymmetric supercapacitors based on ultrathin MnO2 nanosheet/carbon fiber cathodes for wearable electronics, Adv. Energy Mater. 6 (2016) 1–9, https://doi.org/10.1002/aenm.201501458.
[103] Y. Wen, T. Qin, Z. Wang, X. Jiang, S. Peng, J. Zhang, J. Hou, F. Huang, D. He, G. Cao, Self-supported binder-free carbon fibers/MnO2electrodes derived from disposable bamboo chopsticks for high-performance supercapacitors, J. Alloys Compd. 699 (2017) 126–135, https://doi.org/10.1016/j.jallcom.2016.12.330.
[104] T. Cordero-Lanzac, F.J. García-Mateos, J.M. Rosas, J. Rodríguez-Mirasol, T. Cordero, Flexible binderless capacitors based on P- and N-containing fibrous activated carbons from denim cloth waste, Carbon N. Y. 139 (2018) 599–608, https://doi.org/10.1016/j.carbon.2018.06.060.
[105] Z. Fan, J. Yan, T. Wei, L. Zhi, G. Ning, T. Li, F. Wei, Asymmetric supercapacitors based on graphene/MnO2 and activated carbon nanofiber electrodes with high power and energy density, Adv. Funct. Mater. 21 (2011) 2366–2375, https://doi.org/10.1002/adfm.201100058.
[106] L. Bao, J. Zang, X. Li, Flexible Zn2SnO4/MnO2 core/shell nanocable-carbon microfiber hybrid composites for high-performance supercapacitor electrodes, Nano Lett. 11 (2011) 1215–1220, https://doi.org/10.1021/nl104205s.
[107] D. Yu, S. Zhai, W. Jiang, K. Goh, L. Wei, X. Chen, R. Jiang, Y. Chen, Transforming pristine carbon fiber tows into high performance solid-state fiber supercapacitors, Adv. Mater. 27 (2015) 4895–4901, https://doi.org/10.1002/adma.201501948.
[108] S. Jiang, T. Shi, X. Zhan, H. Long, S. Xi, H. Hu, Z. Tang, High-performance all-solid-state flexible supercapacitors based on two-step activated carbon cloth, J. Power Sources 272 (2014) 16–23, https://doi.org/10.1016/j.jpowsour.2014.08.049.
[109] M.F.L.L. De Volder, S.H. Tawfick, R.H. Baughman, A.J. Hart, Carbon nanotubes: present and future commercial applications, Science 339 (6119) (2013) 535–539, https://doi.org/10.1126/science:1222453.

[110] A.G. Pandolfo, A.F. Hollenkamp, Carbon properties and their role in supercapacitors, J. Power Sources 157 (2006) 11–27, https://doi.org/10.1016/j.jpowsour.2006.02.065.
[111] C. Emmenegger, P. Mauron, A. Züttel, C. Nützenadel, A. Schneuwly, R. Gallay, L. Schlapbach, Carbon nanotube synthetisized on metallic substrates, Appl. Surf. Sci. 162–163 (2000) 452–456.
[112] J.H. Chen, W.Z. Li, D.Z. Wang, S.X. Yang, J.G. Wen, Z.F. Ren, Electrochemical characterization of carbon nanotubes as electrode in electrochemical double-layer capacitors, Carbon N. Y. 40 (2002) 1193–1197, https://doi.org/10.1016/S0008-6223(01)00266-4.
[113] S. Talapatra, S. Kar, S.K. Pal, R. Vajtai, L. Ci, P. Victor, M.M. Shaijumon, S. Kaur, O. Nalamasu, P.M. Ajayan, Direct growth of aligned carbon nanotubes on bulk metals, Nat. Nanotechnol. 1 (2006) 112–116, https://doi.org/10.1038/nnano.2006.56.
[114] E. Frackowiak, S. Delpeux, K. Jurewicz, K. Szostak, D. Cazorla-Amoros, F. Beguin, Enhanced capacitance of carbon nanotubes through chemical activation, Chem. Phys. Lett. 361 (2002) 35–41, https://doi.org/10.1016/S0009-2614(02)00684-X.
[115] Z. Qiu, D. He, Y. Wang, X. Zhao, W. Zhao, H. Wu, High performance asymmetric supercapacitors with ultrahigh energy density based on hierarchical carbon nanotubes@NiO core–shell nanosheets and defect-introduced graphene sheets with hole structure, RSC Adv. 7 (2017) 7843–7856, https://doi.org/10.1039/C6RA27369F.
[116] J. Yu, W. Lu, S. Pei, K. Gong, L. Wang, L. Meng, Y. Huang, J.P. Smith, K.S. Booksh, Q. Li, J.H. Byun, Y. Oh, Y. Yan, T.W. Chou, Omnidirectionally stretchable high-performance supercapacitor based on isotropic buckled carbon nanotube films, ACS Nano 10 (2016) 5204–5211, https://doi.org/10.1021/acsnano.6b00752.
[117] S.K. Ujjain, P. Ahuja, R. Bhatia, P. Attri, Printable multi-walled carbon nanotubes thin film for high performance all solid state flexible supercapacitors, Mater. Res. Bull. 83 (2016) 167–171, https://doi.org/10.1016/j.materresbull.2016.06.006.
[118] V. Presser, M. Heon, Y. Gogotsi, Carbide-derived carbons - from porous networks to nanotubes and graphene, Adv. Funct. Mater. 21 (2011) 810–833, https://doi.org/10.1002/adfm.201002094.
[119] K.I. Ozoemena, S. Chen, Nanostructure science and technology nanomaterials in advanced batteries and supercapacitors, Springer International Publishing, 2016 doi: 10.1007/978-3-319-26082-2.
[120] P.C. Gao, W.Y. Tsai, B. Daffos, P.L. Taberna, C.R. Pérez, Y. Gogotsi, P. Simon, F. Favier, Graphene-like carbide derived carbon for high-power supercapacitors, Nano Energy 12 (2015) 197–206, https://doi.org/10.1016/j.nanoen.2014.12.017.
[121] Y. Gogotsi, A. Nikitin, H. Ye, W. Zhou, J.E. Fischer, B. Yi, H.C. Foley, M.W. Barsoum, Nanoporous carbide-derived carbon with tunable pore size, Nat. Mater. 2 (2003) 591–594, https://doi.org/10.1038/nmat957.
[122] L. Weinstein, R. Dash, Supercapacitor carbons: have exotic carbons failed? Mater. Today. 16 (2013) 356–357, https://doi.org/10.1016/j.mattod.2013.09.005.
[123] M. Pohl, H. Kurig, I. Tallo, A. Jänes, E. Lust, Novel sol-gel synthesis route of carbide-derived carbon composites for very high power density supercapacitors, Chem. Eng. J. 320 (2017) 576–587, https://doi.org/10.1016/j.cej.2017.03.081.
[124] T. Thomberg, A. Jänes, E. Lust, Energy and power performance of vanadium carbide derived carbon electrode materials for supercapacitors, J. Electroanal. Chem. 630 (2009) 55–62, https://doi.org/10.1016/j.jelechem.2009.02.015.
[125] E. Tee, I. Tallo, T. Thomberg, A. Jänes, E. Lust, Supercapacitors based on activated silicon carbide-derived carbon materials and ionic liquid, J. Electrochem. Soc. 163 (2016) A1317–A1325, https://doi.org/10.1149/2.0931607jes.
[126] L. Zheng, Y. Wang, X. Wang, N. Li, H. An, H. Chen, J. Guo, The preparation and performance of calcium carbide-derived carbon/polyaniline composite electrode material for supercapacitors, J. Power Sources 195 (2010) 1747–1752, https://doi.org/10.1016/j.jpowsour.2009.09.057.
[127] A. Tolosa, B. Krüner, S. Fleischmann, N. Jäckel, M. Zeiger, M. Aslan, I. Grobelsek, V. Presser, Niobium carbide nanofibers as a versatile precursor for high power supercapacitor and high energy battery electrodes, J. Mater. Chem. A. (2016) 16003–16016, https://doi.org/10.1039/C6TA06224E.
[128] F. Liu, D.F. Xue, Electrochemical energy storage applications of “pristine” graphene produced by non-oxidative routes, Sci. China Technol. Sci. 58 (2015) 1841–1850, https://doi.org/10.1007/s11431-015-5932-y.
[129] V.B. Mohan, K. tak Lau, D. Hui, D. Bhattacharyya, Graphene-based materials and their composites: a review on production, applications and product limitations, Compos. Part B Eng. 142 (2018) 200–220, https://doi.org/10.1016/j.compositesb.2018.01.013.
[130] K. Chen, S. Song, D. Xue, Beyond graphene: materials chemistry toward high performance inorganic functional materials, J. Mater. Chem. A. 3 (2015) 2441–2453, https://doi.org/10.1039/c4ta06989g.
[131] F. Liu, S. Song, D. Xue, H. Zhang, Folded structured graphene paper for high performance electrode materials, Adv. Mater. 24 (2012) 1089–1094, https://doi.org/10.1002/adma.201104691.
[132] M. Pumera, Graphene-based nanomaterials and their electrochemistry, Chem. Soc. Rev. 39 (2010) 4146, https://doi.org/10.1039/c002690p.
[133] Francesco Bonaccorso, Luigi Colombo, Guihua Yu, Meryl Stoller, Valentina Tozzini, Andrea C. Ferrari, Rodney S. Ruoff, Vittorio Pellegrini, Graphene, related two-dimensional crystals, and hybrid systems for energy conversion and storage, Science 347 (6217) (2015) 1246501, https://doi.org/10.1126/science:1246501.
[134] K. Chen, F. Liu, D. Xue, S. Komarneni, Carbon with ultrahigh capacitance when graphene paper meets K 3 Fe(CN) 6, Nanoscale 7 (2015) 432–439, https://doi.org/10.1039/c4nr05919k.
[135] M. Moussa, M.F. El-kady, S. Abdel-azeim, R.B. Kaner, P. Majewski, J. Ma, Compact, flexible conducting polymer/graphene nanocomposites for supercapacitors of high volumetric energy density, Compos. Sci. Technol. 160 (2018) 50–59, https://doi.org/10.1016/j.compscitech.2018.02.033.
[136] K. Chen, S. Song, F. Liu, D. Xue, Structural design of graphene for use in electrochemical energy storage devices, Chem. Soc. Rev. 44 (2015) 6230–6257, https://doi.org/10.1039/c5cs00147a.
[137] Z.-S. Wu, G. Zhou, L.-C. Yin, W. Ren, F. Li, H.-M. Cheng, Graphene/metal oxide composite electrode materials for energy storage, Nano Energy 1 (2012) 107–131, https://doi.org/10.1016/j.nanoen.2011.11.001.
[138] R.P. Panmand, P. Patil, Y. Sethi, S.R. Kadam, M.V. Kulkarni, S.W. Gosavi, N.R. Munirathnam, B.B. Kale, Unique perforated graphene derived from Bougainvillea flowers for high-power supercapacitors: a green approach, Nanoscale 9 (2017) 4801–4809, https://doi.org/10.1039/C7NR00583K.
[139] H. Banda, D. Aradilla, A. Benayad, Y. Chenavier, B. Daffos, L. Dubois, F. Duclairoir, One-step synthesis of highly reduced graphene hydrogels for high power supercapacitor applications, J. Power Sources 360 (2017) 538–547, https://doi.org/10.1016/j.jpowsour.2017.06.033.
[140] H. Yang, S. Kannappan, A.S. Pandian, J.-H. Jang, Y.S. Lee, W. Lu, Graphene supercapacitor with both high power and energy density, 445401, Nanotechnology 28 (2017), https://doi.org/10.1088/1361-6528/aa8948.
[141] A. KM, M. Manoj, B. Jinisha, P. VS, S. Jayalekshmi, Mn3O4/reduced graphene oxide nanocomposite electrodes with tailored morphology for high power supercapacitor applications, Electrochim. Acta. 236, 2017, 424–433. doi: 10.1016/j.electacta.2017.03.167.
[142] P. Hao, Z. Zhao, J. Tian, H. Li, Y. Sang, G. Yu, H. Cai, H. Liu, C.P. Wong, A. Umar, Hierarchical porous carbon aerogel derived from bagasse for high performance supercapacitor electrode, Nanoscale 6 (2014) 12120–12129, https://doi.org/10.1039/C4NR03574G.
[143] X. Lin, H. Lou, W. Lu, F. Xu, R. Fu, D. Wu, High-performance organic electrolyte supercapacitors based on intrinsically powdery carbon aerogels, Chinese Chem. Lett. (2017) 4–7, https://doi.org/10.1016/j.cclet.2017.11.024.
[144] Z. Wu, L. Li, J.M. Yan, X.B. Zhang, Materials design and system construction for conventional and new-concept supercapacitors, Adv. Sci. 4 (2017), https://doi.org/10.1002/advs.201600382.
[145] B. Gao, L. Hao, Q. Fu, L. Su, C. Yuan, X. Zhang, Hydrothermal synthesis and electrochemical capacitance of RuO2??xH2O loaded on benzenesulfonic functionalized MWCNTs, Electrochim. Acta. 55 (2010) 3681–3686, https://doi.org/10.1016/j.electacta.2010.01.112.
[146] C.C. Hu, K.H. Chang, M.C. Lin, Y.T. Wu, Design and tailoring of the nanotubular arrayed architecture of hydrous RuO2 for next generation supercapacitors, Nano Lett. 6 (2006) 2690–2695, https://doi.org/10.1021/nl061576a.
[147] H. Xia, Y.S. Meng, G. Yuan, C. Cui, L. Lu, Symmetric RuO2RuO2 supercapacitor operating at 1.6 V by using a neutral aqueous electrolyte, Electrochem. Solid-State Lett. 15 (2011) A60–A63, https://doi.org/10.1149/2.023204esl.
[148] P. Ahuja, S.K. Ujjain, R. Kanojia, Electrochemical behaviour of manganese & ruthenium mixed oxide@ reduced graphene oxide nanoribbon composite in symmetric and asymmetric supercapacitor, Appl. Surf. Sci. 427 (2017) 102–111, https://doi.org/10.1016/j.apsusc.2017.08.028.
[149] L.Y. Chen, Y. Hou, J.L. Kang, A. Hirata, M.W. Chen, Asymmetric metal oxide pseudocapacitors advanced by three-dimensional nanoporous metal electrodes, J. Mater. Chem. A. 2 (2014) 8448, https://doi.org/10.1039/c4ta00965g.
[150] E. Umeshbabu, P. Justin, G.R. Rao, Tuning the Surface Morphology and Pseudocapacitance of MnO2 by Facile Green Method Employing Organic Reducing Sugars Tuning the Surface Morphology and Pseudocapacitance of MnO 2 by Facile Green Method Employing Organic Reducing Sugars In the present work, 2018. doi: 10.1021/acsaem.8b00390.
[151] C. Xu, F. Kang, B. Li, H. Du, Recent progress on manganese dioxide based supercapacitors, J. Mater. Res. 25 (2010) 1421–1432, https://doi.org/10.1557/jmr.2010.0211.
[152] J. Kang, A. Hirata, L. Kang, X. Zhang, Y. Hou, L. Chen, C. Li, T. Fujita, K. Akagi, M. Chen, Enhanced supercapacitor performance of MnO $_2$ by atomic doping, Angew. Chemie Int. Ed. 52 (2013) 1664–1667, https://doi.org/10.1002/anie.201208993.
[153] L. Peng, X. Peng, B. Liu, C. Wu, Y. Xie, G. Yu, Ultrathin two-dimensional MnO2/graphene hybrid nanostructures for high-performance, flexible planar supercapacitors, Nano Lett. 13 (2013) 2151–2157, https://doi.org/10.1021/nl400600x.
[154] X. Wang, B.D. Myers, J. Yan, G. Shekhawat, V. Dravid, P.S. Lee, Manganese oxide micro-supercapacitors with ultra-high areal capacitance, Nanoscale 5 (2013) 4119, https://doi.org/10.1039/c3nr00210a.
[155] X. Wang, J. Hu, W. Liu, G. Wang, J. An, J. Lian, Ni-Zn binary system hydroxide, oxide and sulfide materials: synthesis and high supercapacitor performance, J. Mater. Chem. A. 3 (2015) 23333–23344, https://doi.org/10.1039/c5ta07169k.
[156] P. Geng, S. Zheng, H. Tang, R. Zhu, L. Zhang, S. Cao, H. Xue, H. Pang, Transition metal sulfides based on graphene for electrochemical energy storage, Adv. Energy Mater. 8 (2018) 1–26, https://doi.org/10.1002/aenm.201703259.
[157] A. Gigot, M. Fontana, M. Serrapede, M. Castellino, S. Bianco, M. Armandi, B. Bonelli, C.F. Pirri, E. Tresso, P. Rivolo, Mixed 1T–2H phase MoS2/reduced graphene oxide as active electrode for enhanced supercapacitive performance, ACS Appl. Mater. Interfaces 8 (2016) 32842–32852, https://doi.org/10.1021/acsami.6b11290.
[158] L. Xu, Y. Lu, One-step synthesis of cobalt sulfide/reduced graphene oxide composite used as electrode material for supercapacitor, RSC Adv. 5 (2015), https://doi.org/10.1039/C5RA11711A.
[159] P.R. Jothi, R.R. Salunkhe, M. Pramanik, S. Kannan, Y. Yamauchi, Surfactant-assisted synthesis of nanoporous nickel sulfide flakes and their hybridization with reduced graphene oxides for supercapacitor applications, RSC Adv. 6 (2016) 21246–21253, https://doi.org/10.1039/c5ra26946f.
[160] J. Yang, C. Yu, X. Fan, S. Liang, S. Li, H. Huang, Z. Ling, C. Hao, J. Qiu,

Electroactive edge site-enriched nickel-cobalt sulfide into graphene frameworks for high-performance asymmetric supercapacitors, Energy Environ. Sci. 9 (2016) 1299–1307, https://doi.org/10.1039/c5ee03633j.
[161] Y. Xiao, D. Su, X. Wang, L. Zhou, S. Wu, F. Li, S. Fang, In suit growth of ultra-dispersed NiCo2S4 nanoparticles on graphene for asymmetric supercapacitors, Electrochim. Acta. 176 (2015) 44–50, https://doi.org/10.1016/j.electacta.2015.06.128.
[162] G.A. Snook, P. Kao, A.S. Best, Conducting-polymer-based supercapacitor devices and electrodes, J. Power Sources 196 (2011) 1–12, https://doi.org/10.1016/j.jpowsour.2010.06.084.
[163] L. Li, Z. Wu, S. Yuan, X.B. Zhang, Advances and challenges for flexible energy storage and conversion devices and systems, Energy Environ. Sci. 7 (2014) 2101–2122, https://doi.org/10.1039/c4ee00318g.
[164] Y. Huang, H. Li, Z. Wang, M. Zhu, Z. Pei, Q. Xue, Y. Huang, C. Zhi, Nanostructured polypyrrole as a flexible electrode material of supercapacitor, Nano Energy. 22 (2016) 422–438, https://doi.org/10.1016/j.nanoen.2016.02.047.
[165] Y. Shi, G. Yu, Designing hierarchically nanostructured conductive polymer gels for electrochemical energy storage and conversion, Chem. Mater. 28 (2016) 2466–2477, https://doi.org/10.1021/acs.chemmater.5b04879.
[166] Y. Shi, L. Pan, B. Liu, Y. Wang, Y. Cui, Z. Bao, G. Yu, Nanostructured conductive polypyrrole hydrogels as high-performance, flexible supercapacitor electrodes, J. Mater. Chem. A. 2 (2014) 6086–6091, https://doi.org/10.1039/c4ta00484a.
[167] Y. Song, T.Y. Liu, X.X. Xu, D.Y. Feng, Y. Li, X.X. Liu, Pushing the cycling stability limit of polypyrrole for supercapacitors, Adv. Funct. Mater. 25 (2015) 4626–4632, https://doi.org/10.1002/adfm.201501709.
[168] F. Meng, Y. Ding, Sub-micrometer-thick all-solid-state supercapacitors with high power and energy densities, Adv. Mater. 23 (2011) 4098–4102, https://doi.org/10.1002/adma.201101678.
[169] B. Zhang, P. Zhou, Y. Xu, J. Lin, H. Li, Y. Bai, J. Zhu, S. Mao, J. Wang, Gravity-assisted synthesis of micro/nano-structured polypyrrole for supercapacitors, Chem. Eng. J. 330 (2017) 1060–1067, https://doi.org/10.1016/j.cej.2017.07.183.
[170] K. Sun, S. Zhang, P. Li, Y. Xia, X. Zhang, D. Du, F.H. Isikgor, J. Ouyang, Review on application of PEDOTs and PEDOT:PSS in energy conversion and storage devices, J. Mater. Sci. Mater. Electron. 26 (2015) 4438–4462, https://doi.org/10.1007/s10854-015-2895-5.
[171] Y. Zhou, H. Xu, N. Lachman, M. Ghaffari, S. Wu, Y. Liu, A. Ugur, K.K. Gleason, B.L. Wardle, Q.M. Zhang, Advanced asymmetric supercapacitor based on conducting polymer and aligned carbon nanotubes with controlled nanomorphology, Nano Energy 9 (2014) 176–185, https://doi.org/10.1016/j.nanoen.2014.07.007.
[172] X. He, W. Yang, X. Mao, L. Xu, Y. Zhou, Y. Chen, Y. Zhao, Y. Yang, J. Xu, All-solid state symmetric supercapacitors based on compressible and flexible free-standing 3D carbon nanotubes (CNTs)/poly(3,4-ethylenedioxythiophene) (PEDOT) sponge electrodes, J. Power Sources 376 (2018) 138–146, https://doi.org/10.1016/j.jpowsour.2017.09.084.
[173] M. Moussa, G. Shi, H. Wu, Z. Zhao, N.H. Voelcker, D. Losic, J. Ma, Development of flexible supercapacitors using an inexpensive graphene/PEDOT/MnO2 sponge composite, Mater. Des. 125 (2017) 1–10, https://doi.org/10.1016/j.matdes.2017.03.075.
[174] R. Liu, S. Il Cho, S.B. Lee, Poly(3,4-ethylenedioxythiophene) nanotubes as electrode materials for a high-powered supercapacitor, Nanotechnology 19 (2008), https://doi.org/10.1088/0957-4484/19/21/215710.
[175] M. Rajesh, C.J. Raj, R. Manikandan, B.C. Kim, S.Y. Park, K.H. Yu, A high performance PEDOT/PEDOT symmetric supercapacitor by facile in-situ hydrothermal polymerization of PEDOT nanostructures on flexible carbon fibre cloth electrodes, Mater. Today Energy 6 (2017) 96–104, https://doi.org/10.1016/j.mtener.2017.09.003.
[176] A. Eftekhari, L. Li, Y. Yang, Polyaniline supercapacitors, J. Power Sources 347 (2017) 86–107, https://doi.org/10.1016/j.jpowsour.2017.02.054.
[177] J. Zhou, L. Yu, W. Liu, X. Zhang, W. Mu, X. Du, Z. Zhang, Y. Deng, High performance all-solid supercapacitors based on the network of ultralong manganese dioxide/polyaniline coaxial nanowires, Sci. Rep. 5 (2015) 1–9, https://doi.org/10.1038/srep17858.
[178] W.-S. Huang, B.D. Humphrey, a G. MacDiarmid, Polyaniline, a novel conducting polymer, J. Chem. Soc. Faraday Trans. 82 (1986) 2385–2400, https://doi.org/10.1039/F19868202385.
[179] Y. Gawli, A. Banerjee, D. Dhakras, M. Deo, D. Bulani, P. Wadgaonkar, M. Shelke, S. Ogale, 3D polyaniline architecture by concurrent inorganic and organic acid doping for superior and robust high rate supercapacitor performance, Sci. Rep. 6 (2016) 1–10, https://doi.org/10.1038/srep21002.
[180] L.J. Bian, F. Luan, S.S. Liu, X.X. Liu, Self-doped polyaniline on functionalized carbon cloth as electroactive materials for supercapacitor, Electrochim. Acta. 64 (2012) 17–22, https://doi.org/10.1016/j.electacta.2011.12.012.
[181] H.R. Ghenaatian, M.F. Mousavi, S.H. Kazemi, M. Shamsipur, Electrochemical investigations of self-doped polyaniline nanofibers as a new electroactive material for high performance redox supercapacitor, Synth. Met. 159 (2009) 1717–1722, https://doi.org/10.1016/j.synthmet.2009.05.014.
[182] K.R. Prasad, N. Munichandraiah, Electrochemical studies of polyaniline in a gel polymer electrolyte, Electrochem. Solid-State Lett. 5 (2002) A271–A274, https://doi.org/10.1149/1.1516910.
[183] P. Li, Z. Jin, L. Peng, F. Zhao, D. Xiao, Y. Jin, G. Yu, Stretchable all-gel-state fiber-shaped supercapacitors enabled by macromolecularly interconnected 3D graphene/nanostructured conductive polymer hydrogels, Adv. Mater. 30 (2018) 1–7, https://doi.org/10.1002/adma.201800124.
[184] C. Wu, X. Lu, L. Peng, K. Xu, X. Peng, J. Huang, G. Yu, Y. Xie, Two-dimensional vanadyl phosphate ultrathin nanosheets for high energy density and flexible pseudocapacitors, Nat. Commun. 4 (2013) 1–7, https://doi.org/10.1038/ncomms3431.
[185] C. Zhang, Q. Zhang, K. Zhang, Z. Xiao, Y. Yang, L. Wang, Facile synthesis of a two-dimensional layered Ni- MOF electrode material for high performance, 2018, 17747–17753. doi: 1 0.1039/c8ra01002a.
[186] J. Yang, C. Zheng, P. Xiong, Y. Li, M. Wei, Zn-doped Ni-MOF material with a high supercapacitive performance, J. Mater. Chem. A. 2 (2014) 19005–19010, https://doi.org/10.1039/c4ta04346d.
[187] K.M. Choi, H.M. Jeong, J.H. Park, Y. Zhang, J.K. Kang, Supercapacitors of nanocrystalline metal À organic frameworks, ACS Nano 8 (2014) 7451–7457, https://doi.org/10.1021/nn5027092.
[188] F. Wang, X. Wu, X. Yuan, Z. Liu, Y. Zhang, L. Fu, Y. Zhu, Q. Zhou, Y. Wu, W. Huang, Latest advances in supercapacitors: from new electrode materials to novel device designs, Chem. Soc. Rev. 6816 (2017) 6816–6854, https://doi.org/10.1039/C7CS00205J.
[189] M. Rubio-Martinez, C. Avci-Camur, A.W. Thornton, I. Imaz, D. Maspoch, M.R. Hill, New synthetic routes towards MOF production at scale, Chem. Soc. Rev. 46 (2017) 3453–3480, https://doi.org/10.1039/c7cs00109f.
[190] A. Mahmood, W. Guo, H. Tabassum, R. Zou, Metal-organic framework-based nanomaterials for electrocatalysis, Adv. Energy Mater. 6 (2016), https://doi.org/10.1002/aenm.201600423.
[191] P.J. Waller, F. Gándara, O.M. Yaghi, Chemistry of covalent organic frameworks, Acc. Chem. Res. 48 (2015) 3053–3063, https://doi.org/10.1021/acs.accounts.5b00369.
[192] M. Ghidiu, M.R. Lukatskaya, M.Q. Zhao, Y. Gogotsi, M.W. Barsoum, Conductive two-dimensional titanium carbide “clay” with high volumetric capacitance, Nature 516 (2015) 78–81, https://doi.org/10.1038/nature13970.
[193] Y. Dall'Agnese, P. Rozier, P.L. Taberna, Y. Gogotsi, P. Simon, Capacitance of two-dimensional titanium carbide (MXene) and MXene/carbon nanotube composites in organic electrolytes, J. Power Sources 306 (2016) 510–515, https://doi.org/10.1016/j.jpowsour.2015.12.036.
[194] O. Mashtalir, M.R. Lukatskaya, A.I. Kolesnikov, E. Raymundo-Piñero, M. Naguib, M.W. Barsoum, Y. Gogotsi, The effect of hydrazine intercalation on the structure and capacitance of 2D titanium carbide (MXene), Nanoscale 8 (2016) 9128–9133, https://doi.org/10.1039/c6nr01462c.
[195] M. Boota, B. Anasori, C. Voigt, M.Q. Zhao, M.W. Barsoum, Y. Gogotsi, Pseudocapacitive electrodes produced by oxidant-free polymerization of pyrrole between the layers of 2D titanium carbide (MXene), Adv. Mater. 28 (2016) 1517–1522, https://doi.org/10.1002/adma.201504705.
[196] Z. Ling, C.E. Ren, M.-Q. Zhao, J. Yang, J.M. Giammarco, J. Qiu, M.W. Barsoum, Y. Gogotsi, Flexible and conductive MXene films and nanocomposites with high capacitance, Proc. Natl. Acad. Sci. 111 (2014) 16676–16681, https://doi.org/10.1073/pnas.1414215111.
[197] A. Maitra, A.K. Das, R. Bera, S.K. Karan, S. Paria, S.K. Si, B.B. Khatua, An approach to fabricate PDMS encapsulated all-solid-state advanced asymmetric supercapacitor device with vertically aligned hierarchical Zn-Fe-Co ternary oxide nanowire and nitrogen doped graphene nanosheet for high power device applications, ACS Appl. Mater. Interfaces. 9 (2017) 5947–5958, https://doi.org/10.1021/acsami.6b13259.
[198] D.P. Dubal, N.R. Chodankar, Z. Caban-Huertas, F. Wolfart, M. Vidotti, R. Holze, C.D. Lokhande, P. Gomez-Romero, Synthetic approach from polypyrrole nanotubes to nitrogen doped pyrolyzed carbon nanotubes for asymmetric supercapacitors, J. Power Sources. 308 (2016) 158–165, https://doi.org/10.1016/j.jpowsour.2016.01.074.
[199] C. Couly, M. Alhabeb, K.L. Van Aken, N. Kurra, L. Gomes, A.M. Navarro-Suárez, B. Anasori, H.N. Alshareef, Y. Gogotsi, Asymmetric flexible mxene-reduced graphene oxide micro-supercapacitor, Adv. Electron. Mater. 4 (2018) 1–8, https://doi.org/10.1002/aelm.201700339.
[200] Z. Li, G. Ma, R. Ge, F. Qin, X. Dong, W. Meng, W. Meng, T. Liu, J. Tong, F. Jiang, Y. Zhou, K. Li, X. Min, K. Huo, Y. Zhou, Free-standingconducting polymer films for high-performance energy devices, Angew. Chem., Int. Ed. (2015) 979–982, https://doi.org/10.1002/ange.201509033.
[201] Q.X. Xia, J. Fu, J.M. Yun, R.S. Mane, K.H. Kim, High volumetric energy density annealed-MXene-nickel oxide/MXene asymmetric supercapacitor, RSC Adv. 7 (2017) 11000–11011, https://doi.org/10.1039/c6ra27880a.
[202] K. Chen, D. Xue, High energy density hybrid supercapacitor: in-situ functionalization of vanadium-based colloidal cathode, ACS Appl. Mater. Interfaces. 8 (2016) 29522–29528, https://doi.org/10.1021/acsami.6b10638.
[203] Y. Jia, H. Wan, L. Chen, H. Zhou, J. Chen, Hierarchical nanosheet-based MoS 2 / graphene nanobelts with high electrochemical energy storage performance, J. Power Sources. 354 (2017) 1–9, https://doi.org/10.1016/j.jpowsour.2017.04.031.
[204] Q. Xie, R. Bao, C. Xie, A. Zheng, S. Wu, Y. Zhang, R. Zhang, P. Zhao, Core-shell N-doped active carbon fiber@graphene composites for aqueous symmetric supercapacitors with high-energy and high-power density, J. Power Sources. 317 (2016) 133–142, https://doi.org/10.1016/j.jpowsour.2016.03.099.
[205] J. Yan, C.E. Ren, K. Maleski, C.B. Hatter, B. Anasori, P. Urbankowski, A. Sarycheva, Y. Gogotsi, Flexible MXene/graphene films for ultrafast supercapacitors with outstanding volumetric capacitance, Adv. Funct. Mater. 27 (2017) 1–10, https://doi.org/10.1002/adfm.201701264.
[206] Z. Sun, S. Firdoz, E. Ying-Xuan Yap, L. Li, X. Lu, Hierarchically structured MnO2 nanowires supported on hollow Ni dendrites for high-performance supercapacitors, Nanoscale 5 (2013) 4379–4387, https://doi.org/10.1039/c3nr00209h.
[207] Yi-Zhou Zhang, Tao Cheng, Yang Wang, Wen-Yong Lai, Huan Pang, Wei Huang, Flexible supercapacitors: a simple approach to Boost Capacitance: flexible supercapacitors based on manganese Oxides@MOFs via chemically induced in situ self-transformation (Adv. Mater. 26/2016), Adv. Mater. 28 (26) (2016) 5241, https://

doi.org/10.1002/adma.201670183.
[208] S. Peng, L. Fan, C. Wei, H. Bao, H. Zhang, W. Xu, J. Xu, Polypyrrole/nickel sulfide/bacterial cellulose nanofibrous composite membranes for flexible supercapacitor electrodes, Cellulose 23 (2016) 2639–2651, https://doi.org/10.1007/s10570-016-0981-3.
[209] L.L. Chen, W. Zhai, L.L. Chen, D. Li, X. Ma, Q. Ai, X. Xu, G. Hou, L. Zhang, J. Feng, P. Si, L. Ci, Nanostructured LiMn2O4composite as high-rate cathode for high performance aqueous Li-ion hybrid supercapacitors, J. Power Sources. 392 (2018) 116–122, https://doi.org/10.1016/j.jpowsour.2018.04.103.
[210] C. Zhou, Y. Zhang, Y. Li, J. Liu, Construction of high-capacitance 3D CoO@Polypyrrole nanowire array electrode for aqueous asymmetric supercapacitor, Nano Lett. 13 (2013) 2078–2085, https://doi.org/10.1021/nl400378j.
[211] M. Hashemi, M.S. Rahmanifar, M.F. El-Kady, A. Noori, M.F. Mousavi, R.B. Kaner, The use of an electrocatalytic redox electrolyte for pushing the energy density boundary of a flexible polyaniline electrode to a new limit, Nano Energy 44 (2018) 489–498, https://doi.org/10.1016/j.nanoen.2017.11.058.
[212] Y. Wang, C. Shen, L. Niu, R. Li, H. Guo, Y. Shi, C. Li, X. Liu, Y. Gong, Hydrothermal synthesis of CuCo 2 O 4 /CuO nanowire arrays and RGO/Fe 2 O 3 composites for high-performance aqueous asymmetric supercapacitors, J. Mater. Chem. A. 4 (2016) 9977–9985, https://doi.org/10.1039/C6TA02950G.
[213] P. Yu, Z. Zhang, L. Zheng, F. Teng, L. Hu, X. Fang, A novel sustainable flour derived hierarchical nitrogen-doped porous carbon/polyaniline electrode for advanced asymmetric supercapacitors, Adv. Energy Mater. 6 (2016) 1–10, https://doi.org/10.1002/aenm.201601111.
[214] L. Niu, Y. Wang, F. Ruan, C. Shen, S. Shan, M. Xu, Z. Sun, C. Li, X. Liu, Y. Gong, In situ growth of NiCo 2 S 4 @Ni 3 V 2 O 8 on Ni foam as a binder-free electrode for asymmetric supercapacitors, J. Mater. Chem. A. 4 (2016) 5669–5677, https://doi.org/10.1039/C6TA00078A.
[215] X. Liang, K. Chen, D. Xue, A flexible and ultrahigh energy density capacitor via enhancing surface/interface of carbon cloth supported colloids, Adv. Energy Mater. 8 (2018) 1–7, https://doi.org/10.1002/aenm.201703329.
[216] Q. Chen, D. Cai, H. Zhan, Construction of reduced graphene oxide nano fi bers and cobalt sul fi de nanocomposite for pseudocapacitors with enhanced performance, J. Alloys Compd. 706 (2017) 126–132, https://doi.org/10.1016/j.jallcom.2017.02.189.
[217] S.J. Patil, J.H. Kim, D.W. Lee, Graphene-nanosheet wrapped cobalt sulphide as a binder free hybrid electrode for asymmetric solid-state supercapacitor, J. Power Sources. 342 (2017) 652–665, https://doi.org/10.1016/j.jpowsour.2016.12.096.
[218] T. Lin, C. Dai, T. Tasi, S. Chou, J. Lin, H. Shen, High-performance asymmetric supercapacitor based on Co 9 S 8/3D graphene composite and graphene hydrogel, Chem. Eng. J. 279 (2015) 241–249, https://doi.org/10.1016/j.cej.2015.05.011.
[219] K.P. Annamalai, L. Liu, Y. Tao, Highly exposed nickel cobalt sulfide–rGO nanoporous structures: an advanced energy-storage electrode material, J. Mater. Chem. A. (2017) 9991–9997, https://doi.org/10.1039/c7ta01735a.
[220] Lemu Girma Beka, Xin Li, Weihua Liu, Nickel Cobalt Sulfide core/shell structure on 3D Graphene for supercapacitor application, Sci. Rep. 7 (1) (2017), https://doi.org/10.1038/s41598-017-02309-8.
[221] R. Zhou, C. Han, X. Wang, Hierarchical MoS 2 -coated three-dimensional graphene network for enhanced supercapacitor performances, J. Power Sources 352 (2017) 99–110, https://doi.org/10.1016/j.jpowsour.2017.03.134.
[222] A. Du Pasquier, A. Laforgue, P. Simon, G.G. Amatucci, J.-F. Fauvarque, A nonaqueous asymmetric hybrid Li[sub 4]Ti[sub 5]O[sub 12]/poly(fluorophenylthiophene) energy storage device, J. Electrochem. Soc. 149 (2002) A302, https://doi.org/10.1149/1.1446081.
[223] M. Acerce, D. Voiry, M. Chhowalla, Metallic 1T phase MoS2 nanosheets as supercapacitor electrode materials, Nat. Nanotechnol. 10 (2015) 313–318, https://doi.org/10.1038/nnano.2015.40.
[224] C. Zheng, X. Zhou, H. Cao, G. Wang, Z. Liu, Synthesis of porous graphene/activated carbon composite with high packing density and large specific surface area for supercapacitor electrode material, J. Power Sources 258 (2014) 290–296, https://doi.org/10.1016/j.jpowsour.2014.01.056.
[225] Z. Niu, P. Luan, Q. Shao, H. Dong, J. Li, J. Chen, D. Zhao, L. Cai, W. Zhou, X. Chen, S. Xie, A “skeleton/skin” strategy for preparing ultrathin free-standing single-walled carbon nanotube/polyaniline films for high performance supercapacitor electrodes, Energy Environ. Sci. 5 (2012) 8726–8733, https://doi.org/10.1039/c2ee22042c.
[226] W.Y. Zou, W. Wang, B.L. He, M.L. Sun, Y.S. Yin, Supercapacitive properties of hybrid films of manganese dioxide and polyaniline based on active carbon in organic electrolyte, J. Power Sources 195 (2010) 7489–7493, https://doi.org/10.1016/j.jpowsour.2010.05.020.
[227] Z. Chen, V. Augustyn, J. Wen, Y. Zhang, M. Shen, B. Dunn, Y. Lu, High-performance supercapacitors based on intertwined CNT/V2O5 nanowire nanocomposites, Adv. Mater. 23 (2011) 791–795, https://doi.org/10.1002/adma.201003658.
[228] C.Y. Foo, A. Sumboja, D.J.H. Tan, J. Wang, P.S. Lee, Flexible and highly scalable V2O5-rGO electrodes in an organic electrolyte for supercapacitor devices, Adv. Energy Mater. 4 (2014) 1–7, https://doi.org/10.1002/aenm.201400236.
[229] J.S. Bonso, A. Rahy, S.D. Perera, N. Nour, O. Seitz, Y.J. Chabal, K.J. Balkus, J.P. Ferraris, D.J. Yang, Exfoliated graphite nanoplatelets-V2O5nanotube composite electrodes for supercapacitors, J. Power Sources. 203 (2012) 227–232, https://doi.org/10.1016/j.jpowsour.2011.09.084.
[230] Y. Wang, W. Lai, N. Wang, Z. Jiang, X. Wang, P. Zou, Z. Lin, H.J. Fan, F. Kang, C.-P.P. Wong, C. Yang, A reduced graphene oxide/mixed-valence manganese oxide composite electrode for tailorable and surface mountable supercapacitors with high capacitance and super-long life, Energy Environ. Sci. 10 (2017) 941–949, https://doi.org/10.1039/c6ee03773a.
[231] A. Balducci, W.A. Henderson, M. Mastragostino, S. Passerini, P. Simon, F. Soavi, Cycling stability of a hybrid activated carbon//poly(3-methylthiophene) supercapacitor with N-butyl-N-methylpyrrolidinium bis(trifluoromethanesulfonyl) imide ionic liquid as electrolyte, Electrochim. Acta. 50 (2005) 2233–2237, https://doi.org/10.1016/j.electacta.2004.10.006.
[232] P. Iamprasertkun, A. Krittayavathananon, M. Sawangphruk, N-doped reduced graphene oxide aerogel coated on carboxyl-modified carbon fiber paper for high-performance ionic-liquid supercapacitors, Carbon N. Y. 102 (2016) 455–461, https://doi.org/10.1016/j.carbon.2015.12.092.
[233] A. Pendashteh, E. Senokos, J. Palma, M. Anderson, J.J. Vilatela, R. Marcilla, Manganese dioxide decoration of macroscopic carbon nanotube fibers: from high-performance liquid-based to all-solid-state supercapacitors, J. Power Sources 372 (2017) 64–73, https://doi.org/10.1016/j.jpowsour.2017.10.068.
[234] Z.S. Wu, K. Parvez, S. Li, S. Yang, Z. Liu, S. Liu, X. Feng, K. Müllen, Alternating stacked graphene-conducting polymer compact films with ultrahigh areal and volumetric capacitances for high-energy micro-supercapacitors, Adv. Mater. 27 (2015) 4054–4061, https://doi.org/10.1002/adma.201501643.
[235] L.Y. Chen, J.L. Kang, Y. Hou, P. Liu, T. Fujita, A. Hirata, M.W. Chen, High-energy-density nonaqueous MnO2@nanoporous gold based supercapacitors, J. Mater. Chem. A. 1 (2013) 9202–9207, https://doi.org/10.1039/c3ta11480e.
[236] S. Sellam, a Hashmi, High rate performance of flexible pseudocapacitors fabricated using ionic-liquid-based proton conducting polymer electrolyte with poly(3, 4-ethylenedioxythiophene):poly(styrene sulfonate) and its hydrous ruthenium oxide composite electrodes, ACS Appl. Mater. Interfaces. 5 (2013) 3875–3883, https://doi.org/10.1021/am4005557.
[237] W. Chen, R.B. Rakhi, H.N. Alshareef, Facile synthesis of polyaniline nanotubes using reactive oxide templates for high energy density pseudocapacitors, J. Mater. Chem. A. 1 (2013) 3315–3324, https://doi.org/10.1039/c3ta00499f.
[238] B. Shen, X. Zhang, R. Guo, J. Lang, J. Chen, X. Yan, Carbon encapsulated RuO2nano-dots anchoring on graphene as an electrode for asymmetric supercapacitors with ultralong cycle life in an ionic liquid electrolyte, J. Mater. Chem. A. 4 (2016) 8180–8189, https://doi.org/10.1039/c6ta02473d.
[239] Q. Cheng, J. Tang, N. Shinya, L.C. Qin, Polyaniline modified graphene and carbon nanotube composite electrode for asymmetric supercapacitors of high energy density, J. Power Sources 241 (2013) 423–428, https://doi.org/10.1016/j.jpowsour.2013.04.105.
[240] X. Zhang, D. Zhao, Y. Zhao, P. Tang, Y. Shen, C. Xu, H. Li, Y. Xiao, High performance asymmetric supercapacitor based on MnO2 electrode in ionic liquid electrolyte, J. Mater. Chem. A. 1 (2013) 3706, https://doi.org/10.1039/c3ta00981e.
[241] C.R. Rawool, N.S. Punde, A.S. Rajpurohit, S.P. Karna, A.K. Srivastava, High energy density supercapacitive material based on a ternary hybrid nanocomposite of cobalt hexacyanoferrate/carbon nanofibers/polypyrrole, Electrochim. Acta. 268 (2018) 411–423, https://doi.org/10.1016/j.electacta.2018.02.111.
[242] InventusPower, Annual Update on Lithium-ion Battery Technology, 2018.
[243] H. Dura, J. Perry, T. Lecacou, F. Markoulidis, C. Lei, S. Khalil, M. Decker, M. Weil, Cost analysis of supercapacitor cell production, 4th Int. Conf. Clean Electr. Power Renew. Energy Resour. Impact, ICCEP 2013 (2013) 516–523, https://doi.org/10.1109/ICCEP.2013.6586902.
[244] InvestmentMine, Ruthenium Prices and Ruthenium Price Charts, (2018). http://www.infomine.com/investment/metal-prices/ruthenium/ (accessed June 21, 2018).
[245] P.H. Wang, T.L. Wang, W.C. Lin, H.Y. Lin, M.H. Lee, C.H. Yang, Enhanced supercapacitor performance using molecular self-assembling polyaniline onto carbon nanoparticles, J. Electroanal. Chem. 810 (2018) 145–153, https://doi.org/10.1016/j.jelechem.2017.12.067.
[246] Z. Lin, E. Goikolea, A. Balducci, K. Naoi, P.L. Taberna, M. Salanne, G. Yushin, P. Simon, Materials for supercapacitors: when Li-ion battery power is not enough, Mater. Today 21 (2018) 419–436, https://doi.org/10.1016/j.mattod.2018.01.035.
[247] K.K. Upadhyay, G. Cha, H. Hildebrand, P. Schmuki, T.M. Silva, M.F. Montemor, M. Altomare, Capacitance response in an aqueous electrolyte of Nb2O5nanochannel layers anodically grown in pure molten o-H3PO4, Electrochim. Acta. 281 (2018) 725–737, https://doi.org/10.1016/j.electacta.2018.06.014.
[248] H.S. Kim, J.B. Cook, H. Lin, J.S. Ko, S.H. Tolbert, V. Ozolins, B. Dunn, Oxygen vacancies enhance pseudocapacitive charge storage properties of MoO3 − x, Nat. Mater. 16 (2016), https://doi.org/10.1038/nmat4810.
[249] J. De Xie, H.Y. Li, T.Y. Wu, J.K. Chang, Y.A. Gandomi, Electrochemical energy storage of nanocrystalline vanadium oxide thin films prepared from various plating solutions for supercapacitors, Electrochim. Acta. 273 (2018) 257–263, https://doi.org/10.1016/j.electacta.2018.04.007.
[250] J.S. Sagu, K.G.U. Wijayantha, A.A. Tahir, The pseudocapacitive nature of CoFe2O4 thin films, Electrochim. Acta. 246 (2017) 870–878, https://doi.org/10.1016/j.electacta.2017.06.110.
[251] M.R. Lukatskaya, S. Kota, Z. Lin, M.Q. Zhao, N. Shpigel, M.D. Levi, J. Halim, P.L. Taberna, M.W. Barsoum, P. Simon, Y. Gogotsi, Ultra-high-rate pseudocapacitive energy storage in two-dimensional transition metal carbides, Nat. Energy 6 (2017) 1–6, https://doi.org/10.1038/nenergy.2017.105.
[252] Z. Lin, D. Barbara, P.L. Taberna, K.L. Van Aken, B. Anasori, Y. Gogotsi, P. Simon, Capacitance of Ti3C2TxMXene in ionic liquid electrolyte, J. Power Sources 326 (2016) 575–579, https://doi.org/10.1016/j.jpowsour.2016.04.035.
[253] E.C. Vermisoglou, M. Giannouri, N. Todorova, T. Giannakopoulou, C. Lekakou, C. Trapalis, Recycling of typical supercapacitor materials, Waste Manag. Res. 34 (2016) 337–344, https://doi.org/10.1177/0734242X15625373.
[254] A. Kwade, J. Diekmann, Recycling of Lithium-Ion Batteries : the LithoRec Way, 2018.
[255] K.M. Winslow, S.J. Laux, T.G. Townsend, A review on the growing concern and

potential management strategies of waste lithium-ion batteries, Resour. Conserv. Recycl. 129 (2018) 263–277, https://doi.org/10.1016/j.resconrec.2017.11.001.
[256] NorthernGraphite, Graphite Pricing, (2018). http://northerngraphite.com/graphite-pricing/ (accessed 22.06.18.).
[257] Graphenea, The Price Of Graphene – Graphenea, (2018). https://www.graphenea.com/pages/graphene-price#.WyzkW6dKjcc (accessed 22.06.18.).
[258] J. Chen, W. Shi, Z. Gao, T. Wang, S. Wang, L. Dong, Q. Yang, C. Xiong, Facile preparation of pristine graphene using urea/glycerol as efficient stripping agents, Nano Res. 11 (2018) 820–830, https://doi.org/10.1007/s12274-017-1691-3.
[259] S.J. Woltornist, A.J. Oyer, J.M.Y. Carrillo, A.V. Dobrynin, D.H. Adamson, Conductive thin films of pristine graphene by solvent interface trapping, ACS Nano 7 (2013) 7062–7066, https://doi.org/10.1021/nn402371c.
[260] M.C. Mbambo, S. Khamlich, T. Khamliche, B.M. Mothudi, M. Maaza, Pulsed Nd:YAG laser assisted fabrication of graphene nanosheets in water, MRS Adv. (2018) 1–8, https://doi.org/10.1557/adv.2018.275.
[261] C. Li, X. Zhang, K. Wang, X. Sun, G. Liu, J. Li, H. Tian, J. Li, Y. Ma, Scalable self-propagating high-temperature synthesis of graphene for supercapacitors with superior power density and cyclic stability, Adv. Mater. 29 (2017) 1–8, https://doi.org/10.1002/adma.201604690.
[262] K. Chen, D. Xue, S. Komarneni, Nanoclay assisted electrochemical exfoliation of pencil core to high conductive graphene thin-film electrode, J. Colloid Interface Sci. 487 (2017) 156–161, https://doi.org/10.1016/j.jcis.2016.10.028.
[263] A. Ajina, Statistical optimization of supercapacitor pilot plant manufacturing and process scale-up, University of Nottingham, 2015.
[264] T. Pandolfo, V. Ruiz, S. Sivakkumar, J. Nerkar, General Properties of Electrochemical Capacitors, in: F. Béguin, E. Frackowiak (Eds.), Supercapacitors Mater. Syst. Appl., 2013: pp. 69–109. doi: 10.1002/9783527646661.
[265] J.S. Sagu, N. York, D. Southee, K.G.U.G.U. Wijayantha, Printed electrodes for flexible, light-weight solid-state supercapacitors – a feasibility study, Circuit World 41 (2015) 80–86, https://doi.org/10.1108/CW-01-2015-0004.
[266] M. Yao, X. Zhao, L. Jin, F. Zhao, J. Zhang, J. Dong, Q. Zhang, High energy density asymmetric supercapacitors based on MOF-derived nanoporous carbon/manganese dioxide hybrids, Chem. Eng. J. 322 (2017) 582–589, https://doi.org/10.1016/j.cej.2017.04.075.
[267] N.L. Torad, M. Hu, Y. Kamachi, K. Takai, M. Imura, M. Naito, Y. Yamauchi, Facile synthesis of nanoporous carbons with controlled particle sizes by direct carbonization of monodispersed ZIF-8 crystals, Chem. Commun. 49 (2013) 2521–2523, https://doi.org/10.1039/c3cc38955c.
[268] W. Yuan, L. Cheng, H. Wu, Y. Zhang, S. Lv, X. Guo, One-step synthesis of 2D-layered carbon wrapped transition metal nitrides from transition metal carbides (MXenes) for supercapacitors with ultrahigh cycling stability, Chem. Commun. 54 (2018) 2755–2758, https://doi.org/10.1039/c7cc09017j.
[269] S.G. Mohamed, I. Hussain, J.-J. Shim, One-step synthesis of hollow C-NiCo $_{2}$ $_{S}$ 4 nanostructures for high-performance supercapacitor electrodes, Nanoscale (2018), https://doi.org/10.1039/C7NR07338K.
[270] M. Peplow, One small step… : Disagreements over the definition of a chemical step underlie much broader questions, Chem. World - R. Soc. Chem. (2017). https://www.chemistryworld.com/opinion/what-counts-as-a-step-during-chemical-synthesis/2500261.article (accessed 27.06.18.).
[271] T. Newhouse, P.S. Baran, R.W. Hoffmann, The economies of synthesis, Chem. Soc. Rev. 38 (2009) 3010–3021, https://doi.org/10.1039/b821200g.
[272] C.D. Lokhande, D.P. Dubal, O.S. Joo, Metal oxide thin film based supercapacitors, Curr. Appl. Phys. 11 (2011) 255–270, https://doi.org/10.1016/j.cap.2010.12.001.
[273] H. Palneedi, J.H. Park, D. Maurya, M. Peddigari, G.T. Hwang, V. Annapureddy, J.W. Kim, J.J. Choi, B.D. Hahn, S. Priya, K.J. Lee, J. Ryu, Laser irradiation of metal oxide films and nanostructures: applications and advances, Adv. Mater. 30 (2018) 1–38, https://doi.org/10.1002/adma.201705148.
[274] A. Queraltó, A. Perez del Pino, M. de la Mata, J. Arbiol, M. Tristany, X. Obradors, T. Puig, Ultrafast epitaxial growth of functional oxide thin films by pulsed laser annealing of chemical solutions, Chem. Mater. (2016), https://doi.org/10.1021/acs.chemmater.6b01968 acs.chemmater.6b01968.
[275] J. Yeo, G. Kim, S. Hong, M.S. Kim, D. Kim, J. Lee, H.B. Lee, J. Kwon, Y.D. Suh, H.W. Kang, H.J. Sung, J.H. Choi, W.H. Hong, J.M. Ko, S.H. Lee, S.H. Choa, S.H. Ko, Flexible supercapacitor fabrication by room temperature rapid laser processing of roll-to-roll printed metal nanoparticle ink for wearable electronics application, J. Power Sources. 246 (2014) 562–568, https://doi.org/10.1016/j.jpowsour.2013.08.012.
[276] J. Ryu, H.-S. Kim, H.T. Hahn, Reactive sintering of copper nanoparticles using intense pulsed light for printed electronics, J. Electron. Mater. 40 (2011) 42–50, https://doi.org/10.1007/s11664-010-1384-0.
[277] N.-R. Kim, J.-H. Lee, S.-M. Yi, Y.-C. Joo, Highly conductive ag nanoparticulate films induced by movable rapid thermal annealing applicable to roll-to-roll processing, J. Electrochem. Soc. 158 (2011) K165, https://doi.org/10.1149/1.3596545.
[278] D. Tobjörk, H. Aarnio, P. Pulkkinen, R. Bollström, A. Määttänen, P. Ihalainen, T. Mäkelä, J. Peltonen, M. Toivakka, H. Tenhu, R. Österbacka, IR-sintering of ink-jet printed metal-nanoparticles on paper, Thin Solid Films. 520 (2012) 2949–2955, https://doi.org/10.1016/j.tsf.2011.10.017.
[279] T. Kumpulainen, J. Pekkanen, J. Valkama, J. Laakso, R. Tuokko, M. Mäntysalo, Low temperature nanoparticle sintering with continuous wave and pulse lasers, Opt. Laser Technol. 43 (2011) 570–576, https://doi.org/10.1016/j.optlastec.2010.08.002.
[280] K. Brousse, S. Nguyen, A. Gillet, S. Pinaud, R. Tan, A. Meffre, K. Soulantica, B. Chaudret, P.L. Taberna, M. Respaud, P. Simon, Laser-scribed Ru organometallic complex for the preparation of RuO2 micro-supercapacitor electrodes on flexible substrate, Electrochim. Acta. 281 (2018) 816–821, https://doi.org/10.1016/j.electacta.2018.05.198.
[281] M.F. El-Kady, R.B. Kaner, Scalable fabrication of high-power graphene micro-supercapacitors for flexible and on-chip energy storage, Nat. Commun. 4 (2013) 1475–1479, https://doi.org/10.1038/ncomms2446.
[282] G. Eda, C. Mattevi, H. Yamaguchi, H. Kim, M. Chhowalla, Insulator to semimetal transition in graphene oxide, J. Phys. Chem. C. 113 (2009) 15768–15771, https://doi.org/10.1021/jp9051402.
[283] J. Lin, Z. Peng, Y. Liu, F. Ruiz-Zepeda, R. Ye, E.L.G. Samuel, M.J. Yacaman, B.I. Yakobson, J.M. Tour, Laser-induced porous graphene films from commercial polymers, Nat. Commun. 5 (2015) 1–8, https://doi.org/10.1038/ncomms6714.
[284] C. Liu, H. Liang, D. Wu, X. Lu, Q. Wang, Direct Semiconductor Laser Writing of Few-Layer Graphene Polyhedra Networks for Flexible Solid-State Supercapacitor, 1800092, 2018, 1–11. doi:10.1002/aelm.201800092.
[285] R. Ye, D.K. James, J.M. Tour, Laser-Induced Graphene (2018), https://doi.org/10.1021/acs.accounts.8b00084.